Journal Pre-proof

Design, synthesis, and biological evaluation of 1,2,5-oxadiazole-3-carboximidamide derivatives as novel indoleamine-2,3-dioxygenase 1 inhibitors

Xiaohan Song, Pu Sun, Jiang Wang, Wei Guo, Yi Wang, Ling-hua Meng, Hong Liu

PII: S0223-5234(20)30026-X

DOI: https://doi.org/10.1016/j.ejmech.2020.112059

Reference: EJMECH 112059

To appear in: *European Journal of Medicinal Chemistry*

Received Date: 23 October 2019

Revised Date: 16 December 2019

Accepted Date: 8 January 2020

Please cite this article as: X. Song, P. Sun, J. Wang, W. Guo, Y. Wang, L.-h. Meng, H. Liu, Design, synthesis, and biological evaluation of 1,2,5-oxadiazole-3-carboximidamide derivatives as novel indoleamine-2,3-dioxygenase 1 inhibitors, *European Journal of Medicinal Chemistry* (2020), doi: https://doi.org/10.1016/j.ejmech.2020.112059.

Title:

Design, synthesis, and biological evaluation of 1,2,5-oxadiazole-3-carboximidamide derivatives as novel indoleamine-2,3-dioxygenase 1 inhibitors

Graphical Abstract

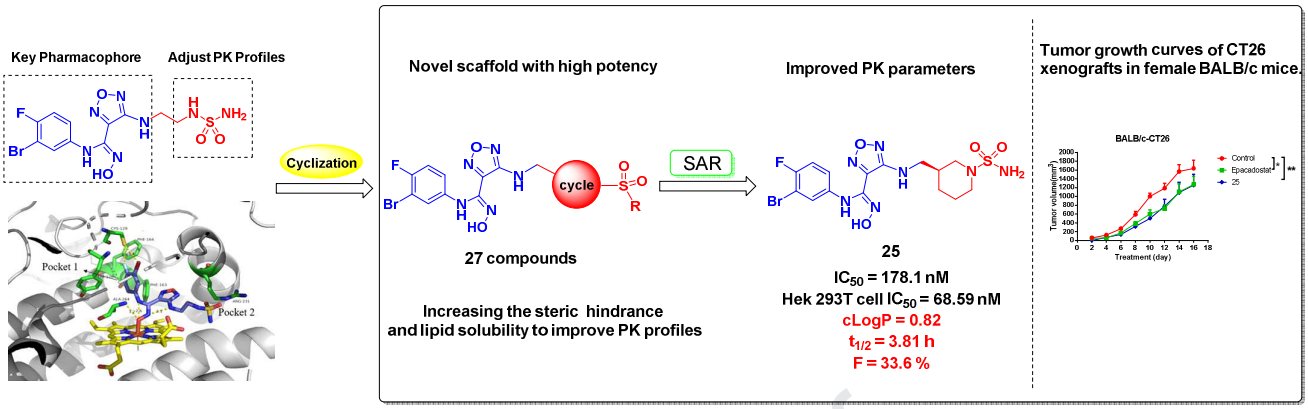

Highlights:

- Novel 1,2,5-oxadiazole-3-carboximidamide derivatives as IDO1 inhibitors were designed, synthesized, and evaluated.
- The structure-activity relationship (SAR) of this novel series of 27 compounds was demonstrated.
- Compound **23**, **25** and **26** demonstrated potent *in vitro* inhibitory activity against hIDO1 (IC_{50} = 108.7, 178.1 and 139.1 nM respectively) and compound **25** showed improved PK profiles ($t_{1/2}$ = 3.81 h, F = 33.6 %) compared with epacadostat.
- Compound **25** exhibited the similar anti-tumor efficacy with epacadostat without inducing significant change in body weight compared to the control group.

Design, synthesis, and biological evaluation of 1,2,5-oxadiazole-3-carboximidamide derivatives as novel indoleamine-2,3-dioxygenase 1 inhibitors

Xiaohan Song,[†,‡,‖] Pu Sun,[#,‡,‖] Jiang Wang,[†,‡] Wei Guo,[#,‡] Yi Wang,[#] Ling-hua Meng,[*,#,‡] and Hong Liu[*,†,‡]

[†] State Key Laboratory of Drug Research and CAS Key Laboratory of Receptor Research, Shanghai Institute of Materia Medica, Chinese Academy of Sciences, 555 Zu Chong Zhi Road, Shanghai, 201203, China.

[#] Division of Anti-Tumor Pharmacology, Shanghai Institute of Materia Medica, Chinese Academy of Sciences, 501 Haike Road, Shanghai, 201203, China.

[‡] University of Chinese Academy of Sciences, No.19A Yuquan Road, Beijing 100049, China.

‖These authors contributed equally to this study.

Corresponding Authors

*H. Liu: Phone, +86-21-50807042; E-mail, hliu@simm.ac.cn.

*L. Meng: Phone, +86-21-50805315; E-mail, lhmeng@simm.ac.cn

Abstract:

Indoleamine 2,3-dioxygenase 1 (IDO1) is the enzyme catalyzing the oxidative metabolism of tryptophan, which accounts for cancer immunosuppression in tumor microenvironment. Several compounds targeting IDO1 have been reported and epacadostat shows strong inhibitory activity against IDO1, which is further studied in clinic trails. However, its pharmacokinetic profiles are not satisfactory. The half-life of epacadostat is 2.4 h in human and dosage is 50 mg BID in the phase III clinic trial. To overcome the shortcomings of epacadostat, structure-based drug design was performed to improve the pharmacokinetic profiles *via* changing the metabolic pathway of epacadostat and to enhance anti-tumor potency. A novel series of 1,2,5-oxadiazole-3-carboximidamide derivatives bearing cycle in the side chain were designed, synthesized, and biologically evaluated for their anti-tumor activity. Most of them exhibited potent activity against hIDO1 in enzymatic assays and in HEK293T cells over-expressing hIDO1. Among them, compound **23**, **25** and **26** showed significant inhibitory activity against hIDO1 (IC_{50} = 108.7, 178.1 and 139.1 nM respectively) and in HEK293T cells expressing hIDO1 (cellular IC_{50} = 19.88, 68.59 and 57.76 nM respectively). Moreover, compound **25** displayed improved PK property with longer half-life ($t_{1/2}$ = 3.81 h in CD-1 mice) and better oral bioavailability (F = 33.6%) compared with epacadostat. In addition, compound **25** showed similar potency to inhibit the growth of CT-26 syngeneic xenograft compared to epacadostat, making it justifiable for further investigation.

Keywords: IDO1 inhibitors, immunotherapy, anti-tumor

INTRODUCTION

Indoleamine 2,3-dioxygenase 1 (IDO1) is a heme-containing protein catalyzing the oxidative metabolism of tryptophan to produce *N*-formylkynurenine [1, 2]. This reaction is the rate limiting step in the kynurenine pathway of tryptophan. It has been reported that tumor cells and immune cells that constitute the tumor microenvironment overexpress IDO1, which is considered to be one of the key factors that result in cancer immunosuppression [3, 4]. Tumor cells and suppressive immune cells could deplete tryptophan that is essential for the T cell differentiation in the tumor microenvironment [5]. As a result, tryptophan depletion activates GCN2 kinase and induces the mid-G1 cell cycle arrest in T cells. However, tumor cells are able to maintain proliferation in the presence of low level of tryptophan [6]. Moreover, accumulation of IDO metabolites also inhibits the function and proliferation of T cell in the tumor microenvironment [7]. For example, kynurenine is a metabolite of tryptophan and it also serves as a ligand of the aryl hydrocarbon receptor (AhR)，which in turn promotes the differentiation of Tregs and suppresses antitumor immune responses [8]. As high expression of IDO1 is associated with poor prognosis in varieties of cancer types, and its important role in immune tolerance, a lot of research has been done towards IDO1 and experimental results indicate that IDO1 inhibition could restore the immune responses in the tumor microenvironment and improve the therapeutic effects of tumor treatment in combination with immune checkpoint inhibitors [5, 9-14].

To date, several types of IDO1 inhibitors, such as epacadostat [15], navoximod [16], BMS-986205 [17] and PF-06840003 [18], have been reported and tested in clinic trials. Compounds **5** [19] and **6** [20] were also proved to be effective IDO1 inhibitors tested in the *in vivo* assays. However, the development of IDO1 inhibitors suffered a setback that the phase III clinical trial of epacadostat in combination with keytruda for advanced melanoma treatment did not reach the primary end point in 2018 [21]. Therefore, pharmaceutical companies reappraise their clinical trials and try to look for a suitable treatment strategy for IDO1 inhibitors. Although the clinical

outcome from a single trail is not the definitive determinant for the field, further exploration for the role of IDO1 serving in the process of tumor immune escape should be done and the development of novel IDO-1 inhibitors is highly needed.

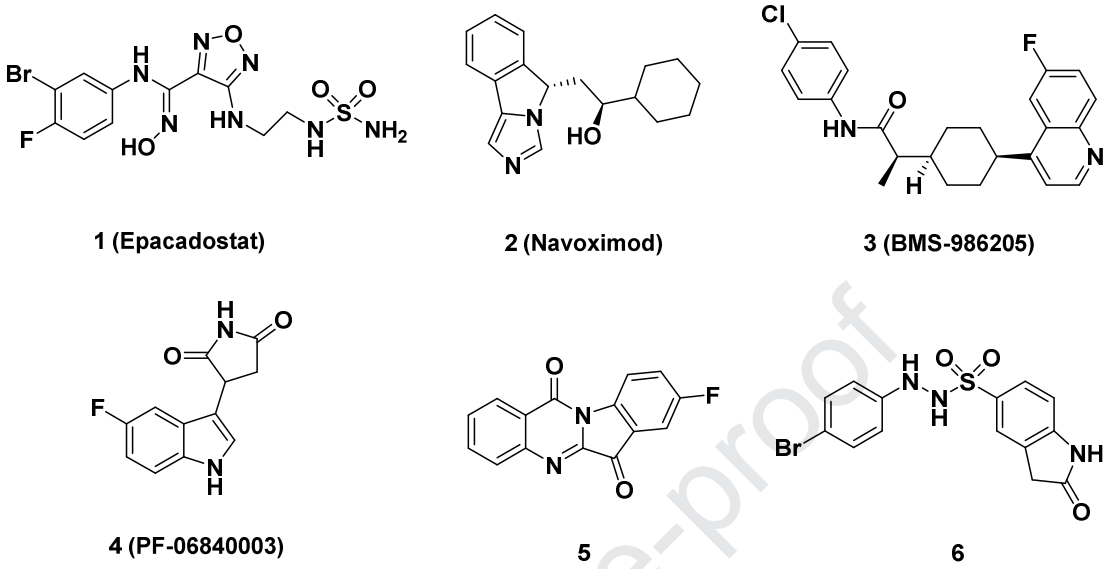

Figure 1. Representative structures of IDO1 inhibitors

Although epacadostat is a well-developed IDO1 inhibitor, its pharmacokinetic profile is not satisfactory. Herein, a series of 1,2,5-oxadiazole-3-carboximidamide derivatives bearing cycle in the side chain were synthesized and evaluated to improve the half-life and oral bioavailability of IDO1 inhibitors by increasing the steric hindrance and lipid solubility. The SAR of new IDO inhibitors was explored and active compounds were tested in the immune-competent animal models.

RESULTS AND DISCUSSION

Design

Epacadostat is quickly consumed by the metabolic enzymes in human, which account for its poor half-life ($t_{1/2}$ = 2.4 h in human). The metabolic study revealed that epacadostat was mainly transformed to *O*-glucuronic acid conjugate compound **M9** by UGT1A9 (Figure 2) [22]. After a single dose of epacadostat in human, the AUC value of **M9** was more than 8-fold greater than that of epacadostat, which lead to poor half-life of epacadostat. Moreover, **M11** was a minor metabolite of epacadostat,

which was produced by gut microbiota and **M12** was a secondary metabolite of epacadostat formed from **M11**. On the other hand, the oral bioavailability of epacadostat is unsatisfactory (F = 11% in rat and F = 33% in cynomolgus), which might result from its poor hydrophobicity (cLogP = 0.09). To overcome these shortcomings, further structural modification of epacadostat is highly desired.

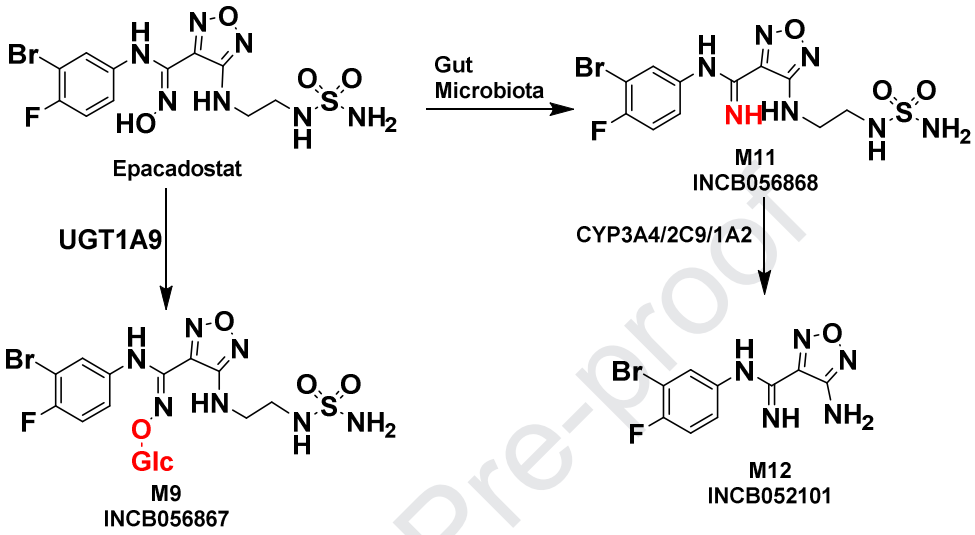

Figure 2. Metabolic pathways of epacadostat in human.

In 2017, Yeh and his coworkers reported the crystal structure of hIDO1 enzyme in complex with epacadostat [23]. As shown in Figure 3, the 3-Br-4-F-phenylamine fragment of epacadostat fulfilled the pocket 1 and the fluoride and bromine group formed halogen bonds with Cys129. The amidoxime group coordinates to the heme iron *via* the oxygen atom, which was of vital importance for stabilizing protein–inhibitor interactions. The furazan and side chain of epacadostat extend into the pocket 2 and the sulfamide group forms electrostatic interaction with Arg231.

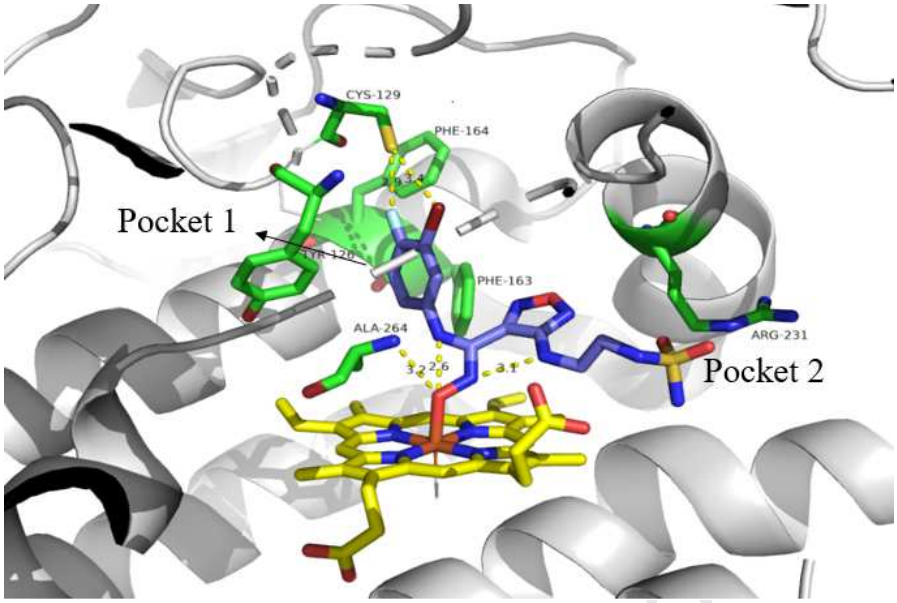

Figure 3. Crystal structure of hIDO1 enzyme in complex with epacadostat

IDO1 (PDB ID: 5WN8, gray) binding pocket for epacadostat (blue carbons), some key interactions are shown as yellow dashed lines.

As aforementioned, the amidoxime group of epacadostat is essential for its inhibitory activity against IDO1 enzyme and the modification of amidoxime group would lead to the decrease of the inhibitory activity against IDO1. As a result, replacing the amidoxime group by bioisosteric groups to avoid the metabolism by UGT1A9 is impracticable. It has been reported that introducing a side chain on the C3 position of furazan could reduce the phase II metabolism, which may cause the collide between the compound and metabolic enzymes [15]. We noticed that the pocket 2 was not fulfilled by epacadostat and the amino group of sulfamide didn't form any hydrogen bond with hIDO1 enzyme, which may be a suitable site to be modified. Therefore, we retained the 1,2,5-oxadiazole-3-carboximidamide fragment and introduced a cycle in the side chain to increase the steric hindrance and lipid solubility, which may improve the PK profiles and biological activity of IDO1 inhibitors (Figure 4). As a result, 1,2,5-oxadiazole-3-carboximidamide derivatives **7-33** were synthesized and evaluated as novel IDO1 inhibitors.

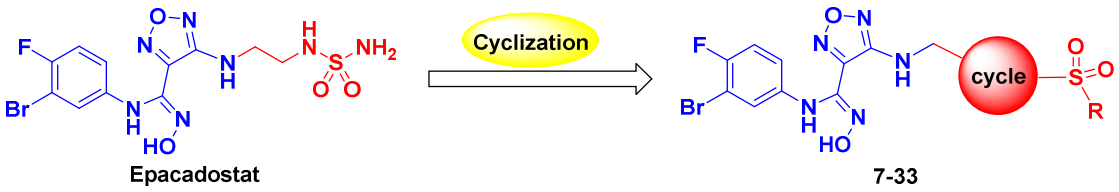

Figure 4. Design of novel IDO inhibitors.

Synthesis of 1,2,5-oxadiazole-3-carboximidamide derivatives

The synthetic route of compounds **7-9**, **19**, **20** and **23-26** is outlined in Scheme 1. Malononitrile **34** was treated with sodium nitrite, hydroxylamine, and hydrochloric acid to afford hydroxyamidine **35**. Then, it was diazotized under acidic condition and reacted with sodium chloride to provide the hydroximoyl chloride **36**, which was further transferred to compound **37** by coupling with 3-Br-4-F-phenylamine. After that, compound **37** was treated with carbonyl diimidazole (CDI) to protect the oxime group, which resulted compound **38**. To introduce the side chain at oxadiazole, compound **38** was oxidized to nitro compound **39**. It was then substituted by a variety of amino compounds (**40a-40k**) and hydrolyzed under acidic condition to afford compounds **41a-41k**. These compounds were further hydrolyzed under acidic condition and reacted with *tert*-butyl (chlorosulfonyl)carbamate to provide compounds **42a-42k**. Finally, target products were obtained *via* a two-step procedure containing acidic and basic hydrolysis.

Scheme 1. Synthesis of the compounds **7-9**, **19**, **20**, and **23-26**.

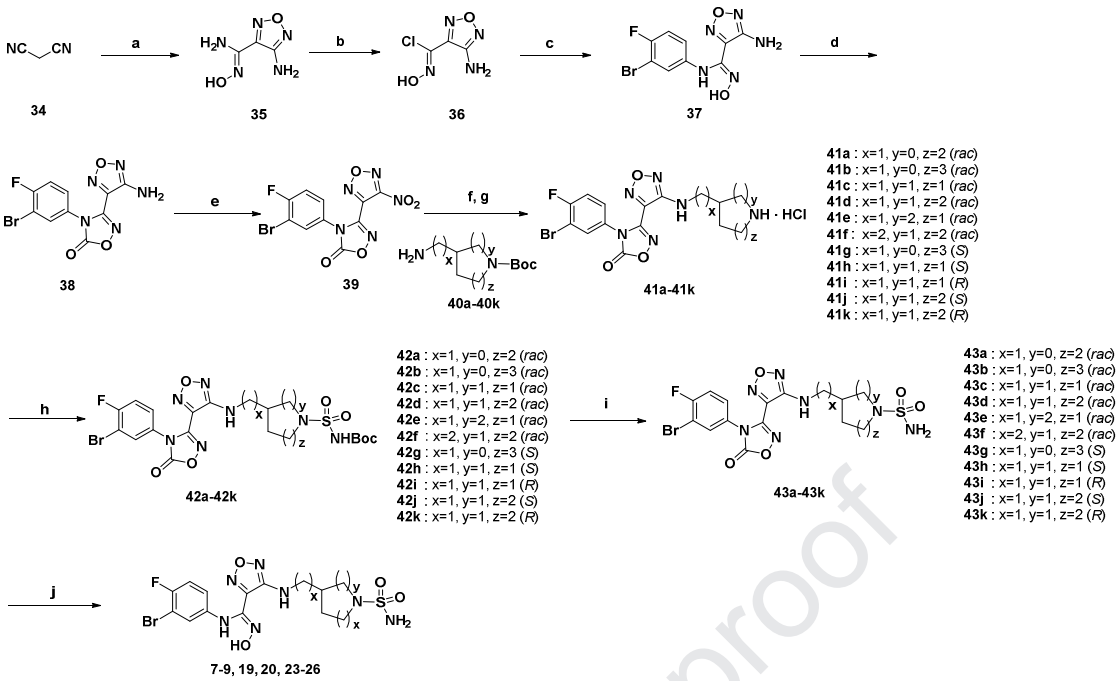

Reagents and conditions: (a) $NaNO_2$, HCl, NH_2OH, H_2O, 100 ^oC (b) $NaNO_2$, HCl, CH_3COOH, NaCl, H_2O, 0 ^oC (c) 3-Br-4-F-phenylamine, $NaHCO_3$, EtOH/H_2O, 60 ^oC (d) CDI, THF, 65 ^oC (e) H_2O_2, TFA, 55 ^oC (f) TEA, THF, r.t. (g) 4 *N* HCl in 1,4-dioxane, CH_2Cl_2, r.t. (h) *tert*-butyl (chlorosulfonyl)carbamate, TEA, THF, 0 ^oC (i) TFA, r.t. (j) NaOH, THF/H_2O, r.t.

Synthetic routes of compounds **10-17**, **21**, **22**, and **27-33** are shown in Scheme 2. Intermediate **39** was substituted by a variety of amino compounds (**44a-44j**) and hydrolyzed under acidic condition to afford compounds **45a-45j**. Then they reacted with alkyl sulfonyl chloride (**46a-46f**) to provide compounds **47aa-47df**. Desired compounds **10-17, 21, 22, 27-33** were obtained after a simple basic hydrolysis of compounds **47aa-47df**.

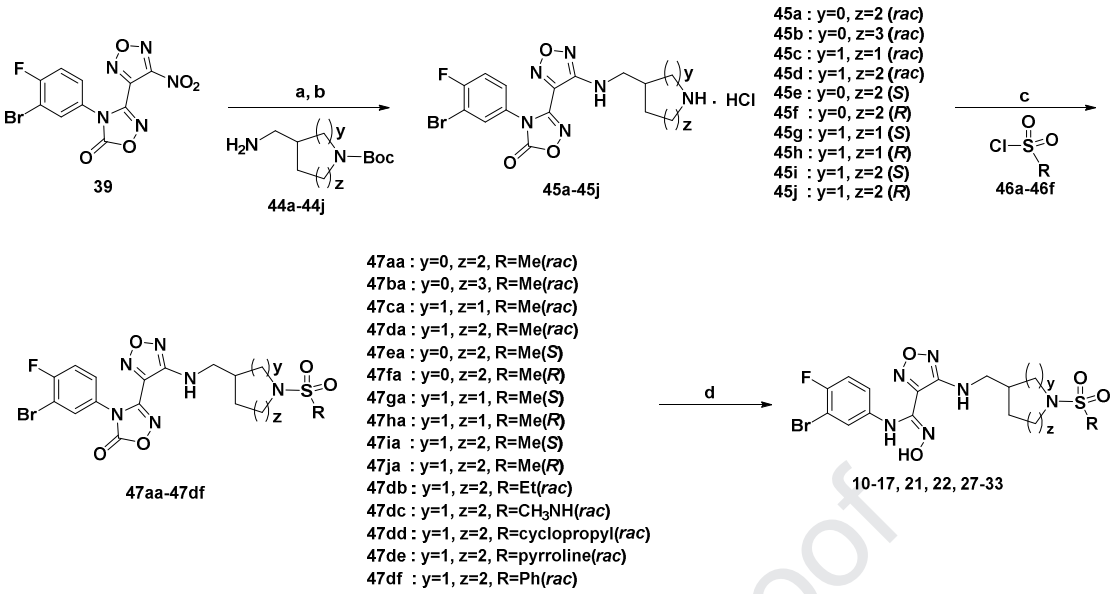

Scheme 2. Synthesis of the compounds **10-17**, **21**, **22**, and **27-33**

Reagents and conditions: (a) TEA, THF, r.t. (b) 4 *N* HCl in 1,4-dioxane, CH_2Cl_2, r.t. (c) TEA, THF, 0 ^oC (d) NaOH, THF/H_2O, r.t.

The synthetic route of compound **18** is very similar to the protocol described in Scheme 1 by replacing compound **40a-40k** with **48**.

Scheme 3. Synthesis of the compound **18**.

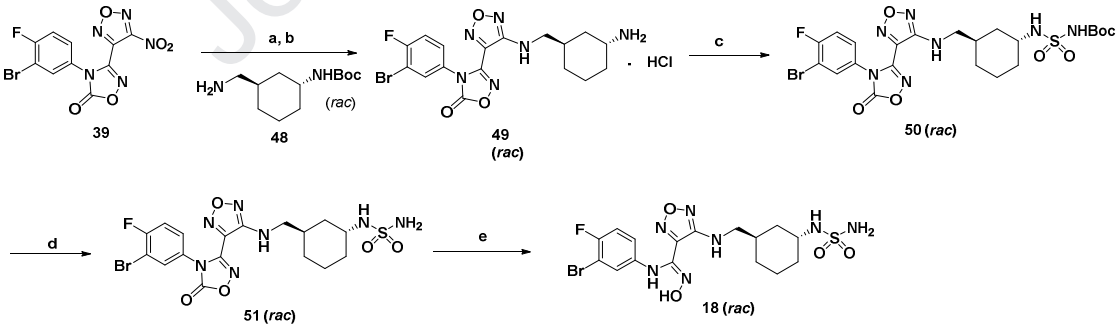

Reagents and conditions: (a) TEA, THF, r.t. (b) 4 *N* HCl in 1,4-dioxane, CH_2Cl_2, r.t. (c) *tert*-butyl (chlorosulfonyl)carbamate, TEA, THF, 0^oC (d) NaOH, THF/H_2O, r.t.

Structure−Activity Relationships of 1,2,5-oxadiazole-3-carboximidamides derivatives

All the synthesized compounds were screened for their activity to inhibit the enzymatic activity of the purified recombinant hIDO1. Dozens of 1,2,5-oxadiazole-3-carboximidamides derivatives were designed and synthesized to explore their structure−activity relationship. The preliminary SAR at the side chain bearing different six-membered cycle was first investigated (compound **7**-**9**). Among them, compound **8** of which the sulfamide was on the *para*-position exhibited a moderate inhibitory activity (IC_{50} = 142 nM) and improvement in lipid solubility (cLogP = 0.82). Analogs **10** and **11** were obtained by replacing the amino of sulfamide with methyl. However, these two compounds showed decreased inhibitory activity against hIDO1 enzyme, which may be due to the lack of interaction with the solvent. Then, difluoromethyl substituted analog **12** were synthesized, which might form electrostatic interaction with Arg231 residue in pocket 2 and possessed better lipid solubility (**12**, cLogP = 2.88). To our disappointment, it displayed less potent inhibitory activity than compound **8** (**12**, IC_{50} = 489.6 nM). Then different substitution of sulfamide which might filled the pocket 2 were investigated. Extending the chain of sulfonyl to yield compounds **13** and **14** resulted in decreased inhibitory activities (**13**, IC_{50} = 517.2 nM; **14**, IC_{50} > 1000 nM). And analogs containing two cycles were prepared for further exploration of SAR. Replacing the amino group of compound **8** by cyclopropyl, pyrroline, or phenyl gave compounds **15-17**, however, none of them displayed satisfactory inhibitory activity (**15**, IC_{50} = 476.9 nM; **16**, IC_{50} = 601.9 nM; **17**, IC_{50} = 585.2 nM). Prolonging the side chain gave compounds **18** and **19**, which were also inferior IDO inhibitors than compound **8** (**18**, IC_{50} = 425.7 nM; **19**, IC_{50} = 359.7 nM). Replacing the piperidine by pyrroline gave compounds **20**-**22**. Among them, compounds **20** and **22** exhibited similar activities with compound **8** (**20**, IC_{50} = 122.8 nM; **22**, IC_{50} = 188.0 nM). Then, enantiomers of compounds **7**, **8**, **10**, **20**, **21**, and **22** were synthesized and evaluated. As shown in Table 1, the *R* enantiomers (**26**, IC_{50} = 139.1 nM; **29**, IC_{50} = 443.3 nM; **31**, IC_{50} = 150.1 nM) demonstrated improvement in inhibitory activity against IDO1 over the *S* enantiomers (**25**, IC_{50} = 178.1 nM; **28**, IC_{50} = 716.8 nM; **30**, IC_{50} = 529.0 nM). However, enantiomer **23** (*S* configuration, IC_{50} = 108.7 nM) is more effective than **24** (*R* configuration, IC_{50} =

146.4 nM) and the two enantiomers of **10** showed similar inhibitory activity (**32**, IC_{50} = 360.3 nM; **33**, IC_{50} = 363.2 nM). The difference in the inhibitory activity might be related to the distance between sulfamide group of compound and Arg231, which formed hydrogen bond to stabilize protein–inhibitor interactions. And enantiomer **24** (IC_{50} = 108.7 nM) showed potent inhibitory activity similar to epacadostat.

Table 1. Inhibitory activity against IDO1 of 1,2,5-oxadiazole-3-carboximidamide derivatives.

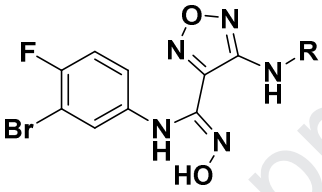

Compd.	R	IC_{50} (nM)	cLogP	Compd.	R	IC_{50} (nM)	cLogP
7	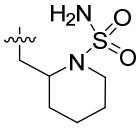	245.2±9.7	1.22	**21**	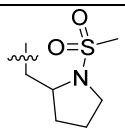	480.1±65.2	1.23
8	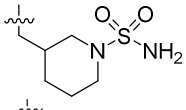	142.5±53.1	0.82	**22**	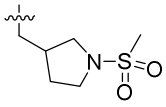	188.0±4.9	0.83
9	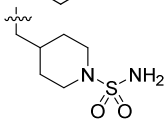	357.8±25.0	0.78	**23**	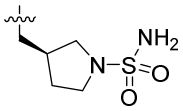	108.7±6.9	0.38
10	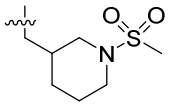	364.1±134.9	1.28	**24**	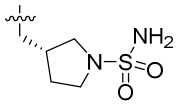	146.4±29.8	0.38
11	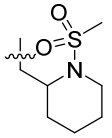	959.5±276.5	1.68	**25**	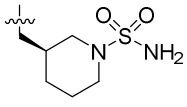	178.1±32.2	0.82
12	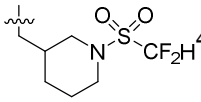	489.6±58.5	2.88	**26**	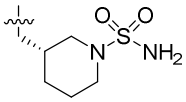	139.1±4.6	0.82
13	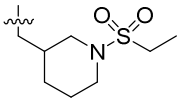	517.2±9.3-	1.79	**27**	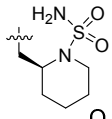	261.7±112.6	1.22
14	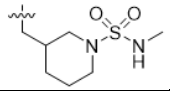	>1000	1.05	**28**	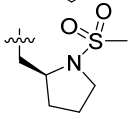	716.8±286.0	1.23

15	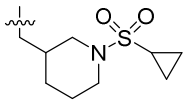	476.9±9.3	2.05	**29**	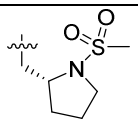	443.3±35.9	1.23
16	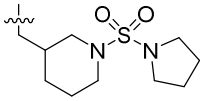	601.9±0.1	1.68	**30**	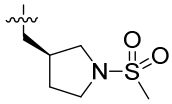	529.0±237.5	0.83
17	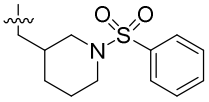	585.2±96.6	3.39	**31**	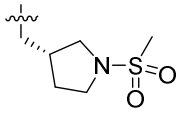	150.1±26.9	0.83
18	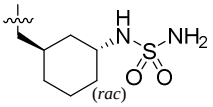	425.7±41.6	1.51	**32**	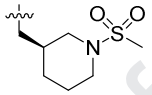	360.3±41.6	1.28
19	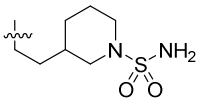	359.7±19.5	1.23	**33**	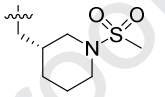	363.2±38.8	1.28
20	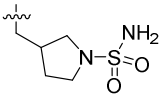	122.8±10.5	0.38	**1**	-	87.4±3.1	0.09

3.2 Inhibitory Activities of the Selected Compounds in HEK 293T cells over-expressing hIDO1

Active compounds (**12**, **15**, **18**, **19**, **23-30**, **32**, and **33**) were further evaluated for their activity in HEK 293T cells over-expressing hIDO1. As shown in Table 2, compounds **12** and **15** displayed weak inhibitory activity in the cell-based assay, indicating that introducing large group might be unbefitting. Compound **23** showed a potent inhibitory activity in the cell-based assay (cellular IC_{50} = 19.88 nM), which was close to the inhibitory activity of epacadostat (cellular IC_{50} = 9.63 nM). Compounds **24**, **25**, **26**, **32**, and **33**, of which the substitution was located on the 3-position of pyrroline or piperidine, also exhibited good potency (cellular IC_{50} = 42.58, 68.59, 57.76, 42.99, and 49.83 nM respectively). Notably, most compounds including epacadostat displayed more potent inhibitory activities in cellular system than those against purified enzyme, which is consistent with other published results [19, 24]. Multiple reasons mentioned in the review by Schwaid and Cornella-Taracido may explain the increased potency in cell-based assay, such as cellular localization, contacts with other proteins or nucleic acids, translational modifications of the protein

and more active metabolites formed in cells [25].

Table 2. Inhibitory activity of derivatives in HEK 293T cells over-expressing hIDO1.

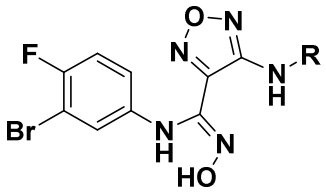

Compd.	R	IC_{50} (nM)	Compd.	R	IC_{50} (nM)
12	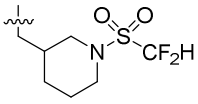	**>** 1000	**26**	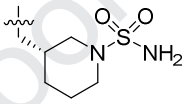	57.76 ± 25.69
15	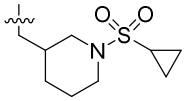	**>** 1000	**27**	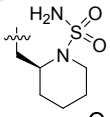	177.35 ± 17.32
18	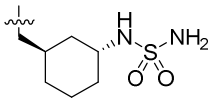	137.95 ± 16.05	**28**	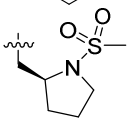	186.20 ± 11.31
19	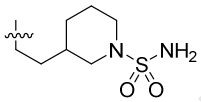	153.75 ± 5.44	**29**	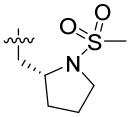	333.65 ± 43.20
23	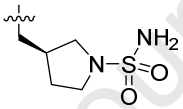	19.88 ± 5.35	**30**	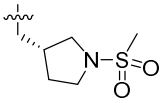	42.99 ± 5.78
24	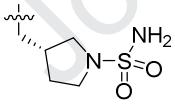	42.58 ± 14.81	**32**	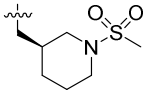	49.83 ± 13.26
25	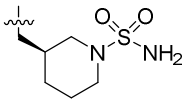	68.59 ± 21.47	**33**	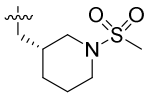	125.44 ± 79.29
1	-	9.63 ± 4.58			

3.3 PK profiles of compounds 23, 25, 26, and epacadostat

To further investigate the effectiveness of design strategy, the pharmacokinetic evaluation of compounds **23**, **25**, **26**, and epacadostat was carried out *via* intravenous (10 mg/kg) and oral administration (20 mg/kg) in CD-1 mice. As shown in table 3, compounds **23** and **26** exhibited similar half-lives (2.81 h and 3.17 h, respectively).

However, these compounds displayed lower bioavailability than that of epacadostat. Compound **25** showed longer half-life ($T_{1/2}$ = 3.81 h) than epacadostat and acceptable oral bioavailability (F = 33.6 %). Meanwhile, it is noteworthy that compound **25** possessed four-fold steady-state volume of distribution than epacadostat (24277 mL/kg and 6319 mL/kg, respectively), which indicated the remarkable enrichment of **25** in extravascular space (e.g., the target tumor tissue).

Table 3. Pharmacokinetic profiles of compounds **23**, **25**, **26**, and epacadostat in CD-1 mice.

	Compd.	$T_{1/2}$ (h)	T_{max} (h)	C_{max} (ng/mL)	AUC_{last} (h*ng/mL)	AUC_{INF_obs} (h*ng/mL)	Cl_{obs} (mL/min/kg)	MRT_{INF_obs} (h)	Vss_{obs} (mL/kg)	F (%)
PO	**23**	2.81	0.25	622	358	392	-	2.65	-	9.70
	25	3.81	0.33	261	588	764		5.10		33.6
	26	3.17	0.333	118	244	304	-	4.91	-	9.84
	Epacadostat	2.59	1.17	343	672	971	-	3.34	-	22.1
IV	**23**	1.19	-	-	1846	1858	90.0	0.622	3356	-
	25	4.09			875	888	195	2.05	24277	-
	26	2.82	-	-	1241	1265	139	1.71	12881	-
	Epacadostat	0.903	-	-	1524	1646	104	1.04	6319	-

3.4 Compound 25 abrogated IDO1-mediated suppression of T cell proliferation and inhibited the growth of colorectal carcinoma CT26 xenografts

It is reported that IDO1 mediate immunosuppression through its capacity to block CD8+T cell proliferation by depleting tryptophan locally [26]. Due to the high potency against hIDO1 *in vitro* and acceptable pharmacokinetic parameters, compound **25** was further evaluated for its effect on T cell proliferation in the presence of tumor cells over-expressing IDO1 by a co-culture assay. Briefly, mouse pancreatic cancer Pan02 cells transfected with pcDNA3.1-IDO1 (Pan02-IDO1) or the

empty plasmid (Pan02-mock) were co-cultured with CD8+T cells labeled with CFSE. T cells were stimulated with IL-2 and dynabeads coated with anti-CD3/anti-CD28. The CD8+T cells were collected and analyzed for proliferation by flow cytometry after 3 days of incubation. Compared to Pan02-mock cells, co-culture of Pan02-IDO1 cells partially suppressed T cell proliferation, which could be completely abrogated in the presence of 100 nM epacadostat or compound **25** (Figure 5a). This result indicated that compound **25** prevented inhibition of $CD8^{+}$T cell proliferation by tumor cells overexpressing IDO1.

The anti-tumor efficacy of compound **25** was further evaluated *in vivo*. Female BALB/c mice bearing established CT26 colorectal tumors were administered orally with compound **25** for 16 days (100 mg/kg, BID) and antitumor efficacy was expressed as tumor growth inhibition (TGI). As shown in Figure 5b and 5c, compound **25** (TGI = 24.5%) exhibited the similar anti-tumor efficacy with epacadostat (TGI = 23.4%) without inducing significant change in body weight compared to the control group.

(a)

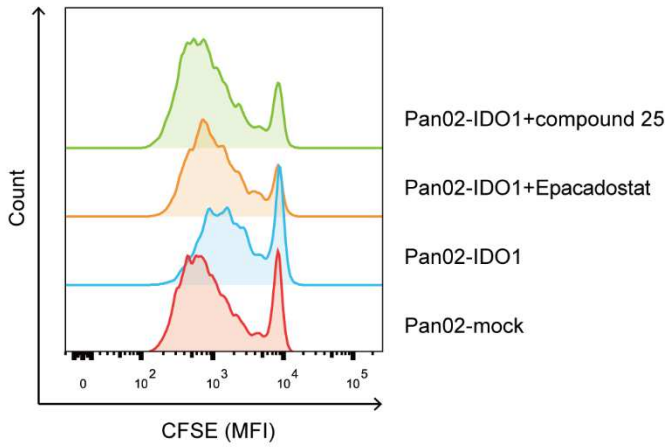

(b)

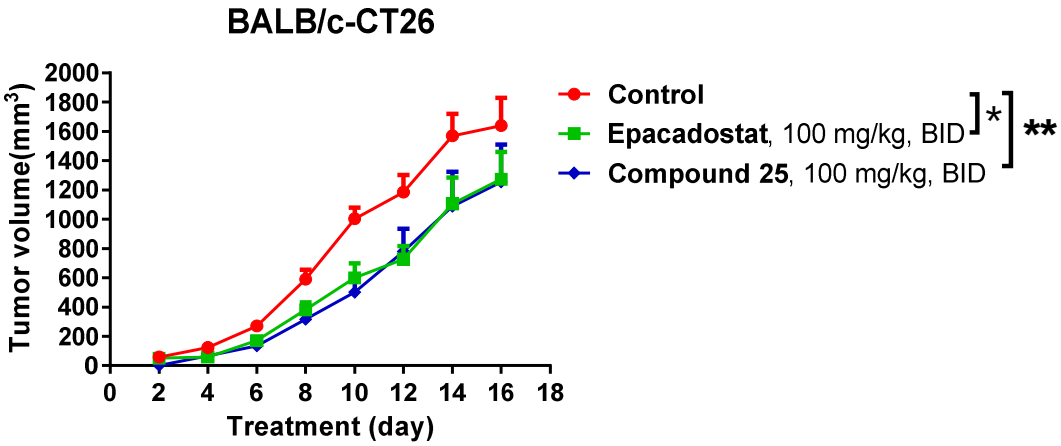

(c)

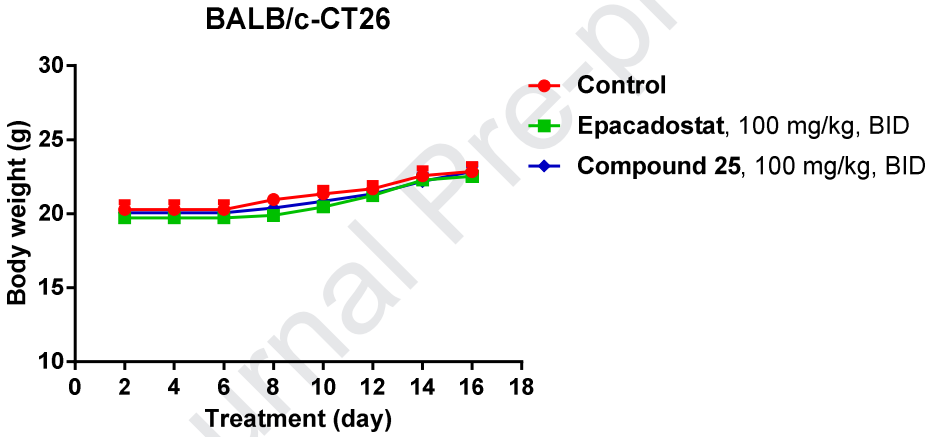

Figure 5. (a) Overlays of CFSE dilution in $CD8^+$T cells after co-culture with Pan02 cells in the presence of 100 nM Compound **25** or epacadostat. Flow cytometry histograms are representatives of two independent experiments. (b)Tumor volume of CT26 xenograft in female BALB/c mice. (Data points represent mean ± SEM.) (c) Body weight of female BALB/c mice.

4. Conclusion

Although epacadostat shows strong inhibitory activity against IDO1 and is further studied in clinic trails., its pharmacokinetic character is not satisfactory. To that point, a cycle in the side chain of epacadostat was introduced aiming to increase the steric hindrance and improve the lipid solubility of compound. Sixteen analogs were synthesized and evaluated to explore the structure-activity relationship and six

analogs of them displayed potent inhibitory activities. The enantiomers of these IDO inhibitors were also evaluated. Compounds **23**, **25**, and **26** exhibited good potency against hIDO1 and IDO1-expressing HEK 293T cells, which were further investigated for their PK profiles. Compound **25** showed improved PK properties with longer half-life and better oral bioavailability compared with epacadostat. Finally, oral administration of compound **25** showed similar therapeutic efficacy with epacadostat in the CT-26 syngeneic xenograft model, which demonstrated that it was suitable for further development as a lead compound.

Experiment Section

hIDO1 enzymatic assay

The effect of the tested compounds on the enzymatic activity of IDO1 was determined as previously described with minor modifications [27]. Briefly, the standard reaction mixture (30 μL) containing potassium phosphate (100 mmol/L, pH 6.5), ascorbic acid neutralized with NaOH (40 mmol/L), catalase (200 μg/mL), methylene blue (20 mmol/L), 0.01% Triton X-100 and rhIDO-1 (0.05 μmol/L) were added to a solution (60 μL) containing the substrate *L*-tryptophan (250 μmol/L) and test compounds at the desired concentration. The reaction was carried out at 37 □ for 30 min and stopped by adding 45 μL of 30% (w/v) trichloroacetic acid. After being heated at 65 □ for 15 min, the reaction mixture was centrifuged at 12000 rpm for 10 min. The supernatant (100 μL) was transferred into a 96-well microplate and mixed with 100 μL of 2% (w/v) *p*-dimethylaminobenzaldehyde (pDMAB) in acetic acid. The yellow pigment derived from kynurenine was measured at 492 nm using a SpectraMax Plus 384 microplate reader (Molecular Devices, Sunnyvale, CA). The IC_{50} values were determined by nonlinear regression analysis with GraphPad Prism 7 software (San Diego, CA, USA).

Cell-based assay of IDO1 activity

The cellular activity of IDO1 was detected as described previously [24]. HEK 293T cells were seeded in a 6-well culture plate at a density of 5×10^5 cells/well. On the second day, HEK 293T cells were transfected with pcDNA3.1-hIDO1 using

Lipofectamine 2000 according to the manufacturer's instructions. The cells were seeded in 96-well microplates at a density of 2.5 × 10^4 cells/well 24 h after transfection and treated with serially diluted tested compounds. After additional 12-h incubation, 200 μL of the culture medium from each well was transferred to a new 96-well plate and mixed with 100 μL of 30% (w/v) trichloroacetic acid. The plate was incubated at 65 □ for 15 min to hydrolyze *N*-formylkynurenine produced by the catalytic reaction of IDO1. The reaction mixture was then centrifuged at 12000 rpm for 10 min and 100 μL of the supernatant was transferred to another 96-well plate and mixed with 100 μL of 2% (w/v) *p*-dimethylaminobenzaldehyde in acetic acid. The yellow pigment derived from kynurenine was measured at 492 nm using a SpectraMax Plus 384 microplate reader (Molecular Devices, Sunnyvale, CA). The IC_{50} values were calculated by using GraphPad Prism 7 software (San Diego, CA, USA).

T cell proliferation assay

Pan02 cells were transfected with pcDNA3.1-hIDO1 or the empty plasmid using Lipofectamine 3000 according to the manufacturer's instructions. After 24 hours, Pan02-IDO1 and Pan02-mock cells were seeded into 6-well plate at a density of 2.5 × 10^5 cells/well. Splenic CD8+T cells were purified by magnetic negative selection (Stem Cell Technologies) and labeled with CFSE (BD Pharmingen). CD8+T cells were co-cultured with Pan02-IDO1 and Pan02-mock cells at a density of 5 × 10^5 cells/well and stimulated with IL-2 (5 ng/ml) and dynabeads coated with anti-CD3/anti-CD28. After 3 days of incubation, CD8+T cells were collected and stained with CD45 (clone 30-F11)-APC-Cy7, CD8 (clone 53-6.7)-APC (BD Pharmingen^{TM}) and 7-amino-actinomycin D (7-AAD; Biolegend) prior to analysis on Fortessa flow cytometer. Data were analyzed with FlowJo.

***In vivo* antitumor activity assay**

Female BALB/c mice (4-6 weeks old) were housed and maintained under specific pathogen-free conditions. Animal procedures were performed according to institutional ethical guidelines of animal care. The murine CT26 colon carcinoma cells were maintained as a monolayer culture in RPMI-1640 medium supplemented

with 10% heat inactivated fetal bovine serum (Gibco product), 100 U/mL penicillin and 100 μg/mL streptomycin at 37 □ in an atmosphere of 5% CO_2. Cells growing in an exponential phase were harvested for tumor inoculation. Each mouse was inoculated subcutaneously at the right lower flank with CT26 cells (0.4×10^6/mouse) in 0.1 mL of PBS. When the tumor volume reached approximately 50 mm^3, the animals were randomly grouped to be administered orally with vehicle or indicated tested compounds twice daily. The tumor sizes and animal weights were measured twice per week using a caliper and weight scale, respectively. The tumor volume (V) was calculated using the formula: V= 0.5 × [length (mm) × $width^2$ (mm^2)].

Chemistry

All reagents (chemicals) were commercially available and used without further purification. Analytical thin-layer chromatography (TLC) was performed on HSGF 254 (0.1 mm thickness). Column chromatography was performed on silica gel 200–300 mesh to purify the compounds. NMR spectra were recorded on Varian-MERCURY Plus-400 and AVANCE III 500 in $CDCl_3$, Methanol-d_4, DMSO-d_6, Acetone-d_6. Chemical shifts were reported in parts per million (ppm, δ) downfield from tetramethylsilane. Proton coupling patterns were described as s = singlet, d = doublet, dd = doublet of doublet, t = triplet, q = quartet, m = multiplet. Low- and high-resolution mass spectra (LRMS and HRMS) were given with electrospray ionization (ESI).

All target compounds **7-33** were confirmed with over 95% purity which were determined by Agilent 1260 HPLC with binary pump, photodiode array detector (DAD), using Agilent Extend-C18 (4.6 × 250 mm, 5 μm), MeOH/H_2O = 70/30 (v/v) at 1.0 mL/min, or Agilent Extend-C18 (4.6 × 250 mm, 5 μm), MeOH/H_2O = 60/40 (v/v) at 1.0 mL/min and calculated the peak areas at 254 nm.

Synthesis of compound **8**

Malononitrile (10 g, 151 mmol) was added to water (200 mL) and stirred for 5 min. The resulting solution was cooled in an ice bath and sodium nitrite (11.8 g, 171

mmol) was added. Then, 10 N hydrochloric acid (10 mL) was added slowly. After 15 min the cold bath was removed and the reaction mixture was stirred for 1.5 h at room temperature. The reaction mixture was cooled to 0°C and 50% aqueous hydroxylamine (30.9 g, 468 mmol) was added all at once. The resulting mixture was stirred for 1 h at room temperature, then it was slowly brought to reflux. Reflux was maintained for 2 h and then the reaction mixture was cooled to room temperature. The reaction mixture was stirred in an ice bath and 6 N hydrochloric acid was added in portions to pH 7.0. Stirring was continued in the ice bath at 5 °C. The precipitate was collected by filtration, washed well with water and dried under vacuum to give the desired product **35** (20 g, 92%). ^{13}C NMR (100 MHz, Methanol-d_4) δ 154.5, 144.4, 139.7.

4-amino-*N*-hydroxy-1,2,5-oxadiazole-3-carbimidoyl chloride (36)

Compound **35** (20 g, 140 mmol) was added to a mixture of water (240 mL), acetic acid (140 mL) and 12 N hydrochloric acid (70 mL) and this suspension was stirred at room temperature until complete solution was achieved. Sodium chloride (23.7 g, 400 mmol) was added and this solution was cool to 0 °C in an ice bath. A solution of sodium nitrite (9.5 g, 140 mmol) in water (30 mL) was added over 1 h. After that, the reaction mixture was stirred in the ice bath for another 1.5 h and then the reaction mixture was warmed to room temperature. The precipitate was collected by filtration, washed well with water and dried under vacuum to give the desired product **36** as a white solid (11 g, 48%).^{13}C NMR (100 MHz, Methanol-d_4) δ 153.8, 141.6, 127.9.

4-amino-*N*-(3-bromo-4-fluorophenyl)-*N*'-hydroxy-1,2,5-oxadiazole-3-carboximidamide (37)

Compound **36** (11 g, 68 mmol) was dissolved in 150 mL EtOH/H_2O (v/v = 5:1). 3-Bromo-4-fluoroaniline (13 g, 68 mmol) and sodium bicarbonate (4.3 g, 41 mmol) were added and stirred for 10 min. Then the mixture was heated to 60 °C and was stirred at 60 °C for 2 hrs. The reaction solution was cooled to room temperature and extracted with ethyl acetate. The combined ethyl acetate solution was dried over

sodium sulfate and concentrated to give the desired product **37** as a white solid (20 g, 93%). ^{13}C NMR (100 MHz, DMSO-d_6) δ 155.6, 154.1 (d, J = 239.1 Hz), 140.8, 139.7, 138.4, 125.2, 121.8 (d, J = 7.3 Hz), 116.4 (d, J = 23.4 Hz), 107.5 (d, J = 22.2 Hz).

3-(4-amino-1,2,5-oxadiazol-3-yl)-4-(3-bromo-4-fluorophenyl)-1,2,4-oxadiazol-5(4*H*)-one (38)

Compound **37** (20 g, 63 mmol) was dissolved in THF. CDI (12 g, 76 mmol) was added to the mixture and stirred for 10 min. The reaction was stirred at 65 °C for 2 hrs. After that, the reaction was concentrated under vacuum. The resulting solid was treated with 1N HCl (100 mL) and stirred for 10 min. The precipitate was collected by filtration, washed well with EtOAc and dried under vacuum to give the desired product **38** as a light yellow solid (16 g,74%). ^{13}C NMR (100 MHz, DMSO-d_6) δ 160.7, 157.2, 156.9 (d, J = 256.1 Hz), 149.3, 134.7, 133.8, 130.5, 129.1, 117.9 (d, J = 23.7 Hz), 108.6 (d, J = 22.6 Hz).

4-(3-bromo-4-fluorophenyl)-3-(4-nitro-1,2,5-oxadiazol-3-yl)-1,2,4-oxadiazol-5(4*H*)-one (39) Compound **38** (16 g, 47 mmol) was dissolved in TFA (100 mL). 30% H_2O_2 solvent (20 mL) was added and stirred for 10 min. Then the mixture was stirred at 55 °C for 48 h. After that, water was added to the mixture and precipitate was collected by filtration. The crude product was purified by silica gel column chromatography to afford product **39** as a yellow solid (5.6 g, 32%). ^{1}H NMR (400 MHz, Chloroform-d) δ 7.68 – 7.55 (m, 1H), 7.39 – 7.19 (m, 2H).

4-(4-bromo-3-fluorophenyl)-3-(4-((piperidin-3-ylmethyl)amino)-1,2,5-oxadiazol-3-yl)-1,2,4-oxadiazol-5(4*H*)-one hydrochloride (41d)

Compound **39** (330 mg, 0.88 mmol) was dissolved in THF (5 mL). *Tert*-butyl 3-(aminomethyl)piperidine-1-carboxylate (225 mg, 1.05 mmol) and TEA (106 mg, 1.05 mmol) were added to the mixture and the reaction was stirred at room temperature for 4 h. After that, 4 *N* HCl in dioxane (2 mL) was added to the mixture and the reaction was stirred for another 1 h. Then the reaction mixture was concentrated under vacuum and the crude product was purified by silica gel column chromatography to afford product **41d** as a white solid (380 mg, 90%). ^{1}H NMR (400 MHz, Methanol-d_4) δ 7.92 (dd, J = 6.0, 2.5 Hz, 1H), 7.60 (ddd, J = 8.8, 4.2, 2.6 Hz,

1H), 7.44 (t, *J* = 8.6 Hz, 1H), 3.44 (dd, *J* = 12.6, 4.0 Hz, 1H), 3.40 – 3.31 (m, 4H), 2.94 (td, *J* = 12.8, 3.2 Hz, 1H), 2.78 (t, *J* = 12.2 Hz, 1H), 2.30 (ddt, *J* = 11.0, 7.3, 4.0 Hz, 1H), 1.96 (d, *J* = 12.8 Hz, 1H), 1.84 – 1.69 (m, 1H), 1.42 – 1.30 (m, 1H).

***Tert*-butyl ((3-(((4-(4-(3-bromo-4-fluorophenyl)-5-oxo-4,5-dihydro-1,2,4-oxadiazol-3-yl)-1,2,5-oxadiazol-3-yl)amino)methyl)piperidin-1-yl)sulfonyl)carbamate (42d)**

Compound **41d** (380 mg, 0.80 mmol) was dissolved in 5 mL dichloromethane followed by the adding of triethylamine (0.148 mL, 1.08 mmol). After cooling to 0 °C, the solution of *tert*-butyl [chlorosulfonyl]carbamate (1 mL, 0.9 mmol) was added to the mixture slowly. After that, the reaction was allowed to warm to 10 °C and stirred at 10 °C for 30 min. Then water (10 mL) was added to the mixture and the layers were separated. The organic layer was washed with brine (10 mL) and the solvents was removed in vacuum. The crude product was purified by silica gel column chromatography to afford product **42d** as a white solid (405 mg, 81%).^{1}H NMR (400 MHz, DMSO-d_6) δ 10.95 (s, 1H), 8.10 (s, 0H), 7.73 (ddd, *J* = 8.9, 4.4, 2.5 Hz, 1H), 7.61 (t, *J* = 8.7 Hz, 1H), 6.72 (t, *J* = 5.9 Hz, 1H), 3.60 (dd, *J* = 12.3, 3.9 Hz, 1H), 3.50 (d, *J* = 12.0 Hz, 1H), 3.24 – 3.11 (m, 2H), 2.87 – 2.74 (m, 1H), 2.61 (dd, *J* = 12.4, 10.1 Hz, 1H), 1.94 (d, *J* = 3.6 Hz, 1H), 1.70 (t, *J* = 17.8 Hz, 2H), 1.43-1.46 (m, 1H)1.42 (s, 9H), 1.14 – 0.99 (m, 1H).

Preparation of *tert*-butyl [chlorosulfonyl]carbamate solution : A 100 mL round bottom flask was charged with chlorosulfonyl isocyanate (1 mL, 11 mmol) and dichloromethane (10 mL). The mixture was cooled to 2 °C and *tert*-Butanol (1 mL, 11 mol) in dichloromethane (1 mL) was added dropwise at a rate so that the temperature did not exceed 10 °C. The resulting solution was stirred at room temperature for 30-60 min to provide *tert*-butyl [chlorosulfonyl]carbamate solution.

***N*-(3-bromo-4-fluorophenyl)-*N*'-hydroxy-4-(((1-sulfamoylpiperidin-3-yl)methyl)amino)-1,2,5-oxadiazole-3-carboximidamide (8)** Compound **42d** (405 mg, 0.78 mmol) was dissolved in 5 mL THF and 5*M* NaOH solution (1 mL, 5.5 mmol) was added. The reaction was stirred for 3h at room temperature. Then 20 mL EtOAc was poured into the mixture and the organic layer was washed by brine for three times.

The desired product **8** was obtained after the purification by silica gel column chromatography as a white solid (265 mg, 69%).

***N*-(3-bromo-4-fluorophenyl)-*N*'-hydroxy-4-(((1-sulfamoylpiperidin-2-yl)methyl)amino)-1,2,5-oxadiazole-3-carboximidamide (7)**

White solid (yield: 53%). HPLC purity: 98.28%. m.p.: 70 - 72 ^{o}C. ^{1}H NMR (500 MHz, DMSO-d_6) δ 11.42 (s, 1H), 8.86 (s, 1H), 7.21 – 7.07 (m, 2H), 6.79 (dt, *J* = 8.9, 3.5 Hz, 1H), 6.66 (s, 2H), 6.18 (dd, *J* = 7.2, 5.1 Hz, 1H), 4.07 (q, *J* = 6.9 Hz, 1H), 3.52 - 3.59 (m, 2H), 3.38 - 3.46 (m, 1H), 2.99 (td, *J* = 10.7, 4.9 Hz, 1H), 1.69 (dt, *J* = 13.6, 6.8 Hz, 1H), 1.54 (q, *J* = 13.9, 13.3 Hz, 5H). ^{13}C NMR (125 MHz, DMSO-d_6) δ 156.2, 154.3 (d, *J* = 237.5 Hz), 140.1, 139.8, 138.4 (d, *J* = 2.8 Hz), 125.3, 122.0 (d, *J* = 7.1 Hz), 116.4 (d, *J* = 23.2 Hz), 107.5 (d, *J* = 22.0 Hz), 51.5, 43.3, 41.3, 25.3, 24.2, 19.0. ESI-MS: m/z 489.7 [M-H]$^{-}$; HRMS (ESI) calculated for C15H19BrFN7O4S [M-H^{+}]: 490.0314; found: 490.0311.

***N*-(3-bromo-4-fluorophenyl)-*N*'-hydroxy-4-(((1-sulfamoylpiperidin-3-yl)methyl)amino)-1,2,5-oxadiazole-3-carboximidamide (8)**

White solid (yield: 49%). HPLC purity: 98.12%. m.p.: 98 - 101 ^{o}C. ^{1}H NMR (400 MHz, DMSO-d_6) δ 11.45 (s, 1H), 8.90 (s, 1H), 7.17 (t, *J* = 8.8 Hz, 1H), 7.11 (dd, *J* = 6.0, 2.7 Hz, 1H), 6.77-6.71 (m, 1H), 6.70 (s, 2H), 6.27 (t, *J* = 5.9 Hz, 1H), 3.39 (dd, *J* = 11.9, 3.3 Hz, 1H), 3.35-3.25 (m ,1H), 3.12 (t, *J* = 6.6 Hz, 2H), 2.53-2.45 (m, 1H), 2.28 (t, *J* = 10.8 Hz, 1H), 1.95-1.83 (m, 1H), 1.77 – 1.65 (m, 1H), 1.65 – 1.57 (m, 1H), 1.44 (q, *J* = 12.0 Hz, 1H), 1.07 – 0.91 (m, 1H). ^{13}C NMR (125 MHz, DMSO-d_6) δ 156.3, 154.3 (d, *J* = 237.5 Hz), 140.4, 139.6, 138.4, 125.4, 122.0 (d, *J* = 6.9 Hz), 116.5 (d, *J* = 23.4 Hz), 107.6 (d, *J* = 22.1 Hz), 50.2, 47.8, 46.9, 35.1, 27.7, 24.0. ESI-MS: m/z 489.8 [M-H]$^{-}$; HRMS (ESI) calculated for C15H19BrFN7O4S [M-H^{+}]:490.0314; found: 490.0319.

***N*-(3-bromo-4-fluorophenyl)-*N*'-hydroxy-4-(((1-sulfamoylpiperidin-4-yl)methyl)amino)-1,2,5-oxadiazole-3-carboximidamide (9)**

White solid (yield: 62%). HPLC purity: 95.66%. m.p.: 147 - 149 °C. ^{1}H NMR (500 MHz, DMSO-d_6) δ 11.46 (s, 1H), 8.89 (s, 1H), 7.19 (t, *J* = 8.7 Hz, 1H), 7.12 (dd, *J* = 6.1, 2.7 Hz, 1H), 6.78 (ddd, *J* = 8.9, 4.2, 2.7 Hz, 1H), 6.69 (s, 2H), 6.28 (t, *J* = 5.9 Hz, 1H), 3.47 (d, *J* = 11.7 Hz, 2H), 3.11 (t, *J* = 6.2 Hz, 2H), 2.50 – 2.43 (m, 2H), 1.74 – 1.63 (m, 2H), 1.31 – 1.07 (m, 3H). ^{13}C NMR (125 MHz, DMSO-d_6) δ 156.2, 154.3 (d, *J* = 237.5 Hz), 140.5, 139.6, 138.4, 125.5, 122.0 (d, *J* = 7.2 Hz), 116.4 (d, *J* = 23.2 Hz), 107.6 (d, *J* = 22.0 Hz), 49.5, 46.2, 34.6, 29.0. ESI-MS: m/z 489.8 [M-H]$^-$; HRMS (ESI) calculated for C15H19BrFN7O4S [M+H$^+$]: 492.0459; found: 492.0466.

_N_-(3-bromo-4-fluorophenyl)-_N'_-hydroxy-4-(((1-(methylsulfonyl)piperidin-3-yl)methyl)amino)-1,2,5-oxadiazole-3-carboximidamide (10)

White solid (yield: 67%). HPLC purity: 99.05%. m.p.: 140 - 142 °C. ^{1}H NMR (600 MHz, DMSO-d_6) δ 11.44 (s, 1H), 8.91 (s, 1H), 7.17 (t, *J* = 8.8 Hz, 1H), 7.11 (dd, *J* = 6.1, 2.7 Hz, 1H), 6.74 (ddd, *J* = 8.9, 4.1, 2.7 Hz, 1H), 6.30 (t, *J* = 6.0 Hz, 1H), 3.48 (dd, *J* = 11.6, 3.8 Hz, 1H), 3.41 (dt, *J* = 11.6, 4.1 Hz, 1H), 3.05 - 3.19 (m, 2H), 2.81 (s, 3H) 2.68 (td, *J* = 11.5, 3.1 Hz, 1H), 2.46 (dd, *J* = 11.6, 10.1 Hz, 1H), 1.89 (ddq, *J* = 10.4, 7.2, 3.5 Hz, 1H), 1.72 (dp, *J* = 13.2, 3.5 Hz, 1H), 1.68 – 1.61 (m, 1H), 1.50 – 1.38 (m, 1H), 1.03 (dtd, *J* = 12.9, 11.2, 3.8 Hz, 1H). ^{13}C NMR (150 MHz, DMSO-d_6) δ 156.4, 154.3 (d, *J* = 237.5 Hz), 140.5, 139.5, 138.3 (d, *J* = 2.8 Hz), 125.4 , 122.0 (d, *J* = 7.1 Hz), 116.5 (d, *J* = 23.2 Hz), 107.6 (d, *J* = 22.0 Hz), 49.5, 47.5, 46.4, 35.3, 34.3, 27.6, 24.3. ESI-MS: m/z 489.7 [M-H]$^-$; HRMS (ESI) calculated for C16H20BrFN6O4S [M+H$^+$]: 491.0507; found: 491.0513.

_N_-(3-bromo-4-fluorophenyl)-_N'_-hydroxy-4-(((1-(methylsulfonyl)piperidin-2-yl)methyl)amino)-1,2,5-oxadiazole-3-carboximidamide (11)

White solid (yield: 43%). HPLC purity: 96.91%. m.p.: 85 - 87 °C. ^{1}H NMR (600 MHz, DMSO-d_6) δ 11.60 – 11.32 (m, 1H), 8.87 (s, 1H), 7.14 (t, *J* = 8.7 Hz, 1H), 7.10 (dd, *J* = 6.1, 2.7 Hz, 1H), 6.74 (ddd, *J* = 8.9, 4.1, 2.7 Hz, 1H), 6.27 (t, *J* = 6.3 Hz, 1H), 4.22 – 3.99 (m, 1H), 3.53-3.59 (m, 2H), 3.35 (dt, *J* = 13.5, 6.6 Hz, 1H), 3.13 – 3.03 (m, 1H), 2.91 (s, 3H), 1.50-1.60 (m, 5H), 1.39 (ddt, *J* = 19.9, 12.2, 5.6 Hz, 1H). ^{13}C NMR (150 MHz, DMSO-d_6) δ 156.1, 154.2 (d, *J* = 237.5 Hz), 140.4, 139.7, 138.4 (d, *J* =

2.8 Hz), 125.3, 121.9 (d, *J* = 6.9 Hz), 116.4 (d, *J* = 23.2 Hz), 107.6 (d, *J* = 22.0 Hz), 50.7, 43.6, 40.8, 40.6, 25.9, 25.0, 18.9. ESI-MS: m/z 489.7 $[M-H]^-$; HRMS (ESI) calculated for C16H20BrFN6O4S $[M+H^+]$: 491.0507; found: 491.0497.

_N_-(3-bromo-4-fluorophenyl)-4-(((1-((difluoromethyl)sulfonyl)piperidin-3-yl)methyl)amino)-_N'_-hydroxy-1,2,5-oxadiazole-3-carboximidamide (12)

White solid (yield: 47%). HPLC purity: 95.10%. m.p.: 65 - 67 ^oC. ^1H NMR (600 MHz, DMSO-d_6) δ 11.46 (s, 1H), 8.92 (s, 1H), 7.15 (t, *J* = 8.7 Hz, 1H), 7.11 (dd, *J* = 6.1, 2.7 Hz, 1H), 7.08 (t, *J* = 52.8 Hz), 6.73 (ddd, *J* = 8.9, 4.1, 2.7 Hz, 1H), 6.34 (t, *J* = 6.1 Hz, 1H), 3.67 (dd, *J* = 12.9, 4.0 Hz, 1H), 3.62 (dd, *J* = 12.6, 3.8 Hz, 1H), 3.12 (h, *J* = 7.1 Hz, 2H), 3.07 – 3.00 (m, 1H), 2.83 (dd, *J* = 12.8, 10.3 Hz, 1H), 1.87 (ddp, *J* = 10.4, 7.1, 3.3 Hz, 1H), 1.77 – 1.64 (m, 2H), 1.48 – 1.34 (m, 1H), 1.14 (dddt, *J* = 16.5, 12.4, 5.3, 3.3 Hz, 1H). ^{13}C NMR (150 MHz, DMSO-d_6) δ 156.3, 154.3(d, *J* = 237.5 Hz), 140.5, 139.4, 138.3, 125.4, 121.9 (d, *J* = 7.1 Hz), 114.7 (t, *J* = 277.5 Hz), 113.8 (d, *J* = 278.0 Hz), 107.6 (d, *J* = 22.1 Hz), 49.8, 47.1, 46.9, 35.7, 27.2, 24.9. ^{19}F NMR (470 MHz, Methenol-d_4) δ -117.7, -124.11. ESI-MS: m/z 542.8 $[M-H]^-$; HRMS (ESI) calculated for C16H17BrF4N6O4S $[M+H^+]$: 545.0224; found: 545.0223.

_N_-(3-bromo-4-fluorophenyl)-4-(((1-(ethylsulfonyl)piperidin-3-yl)methyl)amino)-_N'_-hydroxy-1,2,5-oxadiazole-3-carboximidamide (13)

White solid (yield: 63%). HPLC purity: 96.80%. m.p. : 139 - 141 ^oC. ^1H NMR (500 MHz, DMSO-d_6) δ 11.48 (s, 1H), 8.89 (s, 1H), 7.18 (t, *J* = 8.8 Hz, 1H), 7.13 (dd, *J* = 6.1, 2.7 Hz, 1H), 6.77 (dt, *J* = 9.0, 3.4 Hz, 1H), 6.31 (t, *J* = 6.0 Hz, 1H), 3.53 (dd, *J* = 11.9, 3.8 Hz, 1H), 3.46 – 3.48 (m, 1H), 3.21 – 3.10 (m, 2H), 3.00 (q, *J* = 7.3 Hz, 2H), 2.80 (td, *J* = 11.4, 2.7 Hz, 1H), 2.59 (dd, *J* = 11.9, 9.9 Hz, 1H), 1.88 (dtq, *J* = 13.8, 7.0, 3.5 Hz, 1H), 1.79 – 1.59 (m, 2H), 1.43 (qd, *J* = 10.8, 4.1 Hz, 1H), 1.20 (t, *J* = 7.4 Hz, 3H), 1.09 (td, *J* = 10.8, 7.7 Hz, 1H). ^{13}C NMR (125 MHz, DMSO-d6) δ 156.3, 154.3 (d, *J* = 237.5 Hz), 140.5, 139.6, 138.3 (d, *J* = 2.8 Hz), 125.4, 122.0 (d, *J* = 6.9 Hz), 116.4 (d, *J* = 23.1 Hz), 107.6 (d, *J* = 22.0 Hz), 49.3, 47.4, 46.3, 43.0, 35.6, 27.6, 24.6, 8.0.

ESI-MS: m/z 502.9 [M-H]$^-$; HRMS (ESI) calculated for C16H20BrFN6O4S [M-H$^+$]: 503.0518; found: 503.0522.

N-(3-bromo-4-fluorophenyl)-N'-hydroxy-4-(((1-(N-methylsulfamoyl)piperidin-3-yl)methyl)amino)-1,2,5-oxadiazole-3-carboximidamide (14)

White solid (yield: 62%). HPLC purity: 98.27%. m.p.: 160 – 162 ^{o}C. ^{1}H NMR (400 MHz, DMSO-d_6) δ 11.48 (s, 1H), 8.94 (s, 1H), 7.18 (t, J = 8.8 Hz, 1H), 7.13 (dd, J = 6.1, 2.7 Hz, 1H), 7.06 (q, J = 4.9 Hz, 1H), 6.77 (ddd, J = 8.9, 4.2, 2.7 Hz, 1H), 3.45 (dd, J = 11.9, 3.8 Hz, 1H), 3.33 – 3.39 (m, 1H), 3.20 – 3.08 (m, 2H), 2.67 (td, J = 11.4, 2.7 Hz, 1H), 2.49 (d, J = 4.9 Hz, 4H), 2.47 - 2.52 (m, 1H), 1.89 (ddt, J = 10.2, 6.7, 3.4 Hz, 1H), 1.76 – 1.59 (m, 2H), 1.52 – 1.38 (m, 1H), 1.12 – 0.98 (m, 1H). ^{13}C NMR (100 MHz, DMSO-d_6) δ 156.3, 154.2 (d, *J* = 239.5 Hz), 140.4, 139.5, 138.3, 125.4 , 121.9 (d, *J* = 6.8 Hz), 116.4 (d, *J* = 23.2 Hz), 107.5 (d, *J* = 22.1 Hz), 49.6, 47.5, 46.5, 35.2, 29.4, 27.6, 24.2. ESI-MS: m/z 503.9 [M-H]$^-$; HRMS (ESI) calculated for C16H21BrFN7O4S [M-H$^+$]: 504.0470; found: 504.0487.

***N*-(3-bromo-4-fluorophenyl)-4-(((1-(cyclopropylsulfonyl)piperidin-3-yl)methyl)amino)-*N*'-hydroxy-1,2,5-oxadiazole-3-carboximidamide (15)**

White solid (yield: 49%). HPLC purity: 95.45%. m.p.: 128 - 130 ^{o}C.^{1}H NMR (500 MHz, DMSO-d_6) δ 11.43 (s, 1H), 8.91 (s, 1H), 7.19 (t, *J* = 8.8 Hz, 1H), 7.13 (dd, *J* = 6.0, 2.7 Hz, 1H), 6.77 (ddd, *J* = 9.0, 4.2, 2.7 Hz, 1H), 6.32 (t, *J* = 6.0 Hz, 1H), 3.55 (dd, *J* = 11.9, 3.7 Hz, 1H), 3.49 (dd, *J* = 10.0, 5.9 Hz, 1H), 3.15 (td, *J* = 6.6, 3.7 Hz, 2H), 2.82 (td, *J* = 11.5, 2.8 Hz, 1H), 2.60 (dd, *J* = 11.8, 10.1 Hz, 1H), 2.56 – 2.52 (m, 1H), 1.91 (ddd, *J* = 10.4, 6.8, 3.6 Hz, 1H), 1.71 (ddt, *J* = 23.8, 13.2, 3.8 Hz, 2H), 1.46 (tdt, *J* = 10.9, 7.1, 3.6 Hz, 1H), 1.09 (qd, *J* = 11.3, 3.5 Hz, 1H), 0.96 (dt, *J* = 8.0, 3.1 Hz, 2H), 0.90 (tt, *J* = 4.8, 2.6 Hz, 2H). ^{13}C NMR (125 MHz, DMSO-d_6) δ 156.4, 154.3 (d, *J* = 239.5 Hz), 140.5, 139.5, 138.4, 125.4, 122.0 (d, *J* = 7.0 Hz), 116.5 (d, *J* = 23.5 Hz), 107.6 (d, *J* = 22.3 Hz), 49.9, 47.5, 46.8, 35.5, 27.6, 25.6, 24.5, 4.3. ESI-MS: m/z 515.0 [M-H$^+$]. HRMS (ESI) calculated for C18H22BrFN6O4S [M+H+]:

517.0663; found: 517.0675.

***N*-(3-bromo-4-fluorophenyl)-*N*'-hydroxy-4-(((1-(pyrrolidin-1-ylsulfonyl)piperidin-3-yl)methyl)amino)-1,2,5-oxadiazole-3-carboximidamide (16)**

White solid (yield: 36%). HPLC purity: 95.27%. m.p.： 166 – 168 ^{o}C. ^{1}H NMR (500 MHz, DMSO-d_6) δ 11.48 (s, 1H), 8.89 (s, 1H), 7.18 (t, *J* = 8.8 Hz, 1H), 7.12 (dd, *J* = 6.1, 2.7 Hz, 1H), 6.77 (ddd, *J* = 9.0, 4.1, 2.7 Hz, 1H), 6.33 (t, *J* = 6.0 Hz, 1H), 3.47 (dd, *J* = 12.4, 4.2 Hz, 2H), 3.22 – 3.07 (m, 6H), 2.77 (td, *J* = 11.5, 2.7 Hz, 1H), 2.57 (dd, *J* = 11.9, 10.0 Hz, 1H), 1.88 (ddd, *J* = 10.4, 6.8, 3.5 Hz, 1H), 1.86 – 1.76 (m, 4H), 1.75 – 1.61 (m, 2H), 1.43 (tdd, *J* = 11.6, 5.9, 3.0 Hz, 1H), 1.08 (qd, *J* = 12.0, 11.3, 3.2 Hz, 1H). ^{13}C NMR (125 MHz, DMSO-d_6) δ 156.3, 154.3 (d, *J* = 239.5 Hz), 140.4, 139.5, 138.4 (d, *J* = 2.9 Hz), 125.4, 121.9 (d, *J* = 7.0 Hz), 116.4 (d, *J* = 23.2 Hz), 107.6 (d, *J* = 22.0 Hz), 49.9, 48.5, 47.4, 46.9, 35.4, 27.6, 25.6, 24.4. ESI-MS: m/z 543.9 [M-H]$^{-}$. HRMS (ESI) calculated for C19H25BrFN7O4S [M+H^{+}]: 546.0929; found: 546.0937.

***N*-(3-bromo-4-fluorophenyl)-*N*'-hydroxy-4-(((1-(phenylsulfonyl)piperidin-3-yl)methyl)amino)-1,2,5-oxadiazole-3-carboximidamide (17)**

White solid (yield: 66%). HPLC purity: 95.46%. m.p.： 194 - 196 ^{o}C. ^{1}H NMR (600 MHz, DMSO-d_6) δ 11.45 (s, 1H), 8.91 (s, 1H), 7.74 – 7.67 (m, 3H), 7.66 – 7.58 (m, 2H), 7.19 – 7.03 (m, 2H), 6.74 (ddd, *J* = 8.9, 4.2, 2.7 Hz, 1H), 6.30 (t, *J* = 6.0 Hz, 1H), 3.49 (dd, *J* = 11.6, 3.7 Hz, 1H), 3.47 – 3.41 (m, 2H), 3.07 (dh, *J* = 19.9, 6.4 Hz, 2H), 2.27 (td, *J* = 11.4, 3.0 Hz, 1H), 2.08 (t, *J* = 10.8 Hz, 1H), 1.87 (ddq, *J* = 10.4, 7.2, 4.0, 3.6 Hz, 1H), 1.66 (dt, *J* = 12.9, 3.7 Hz, 1H), 1.54 (dt, *J* = 13.4, 4.1 Hz, 1H), 1.48 – 1.29 (m, 1H), 0.98 – 0.74 (m, 1H). ^{13}C NMR (150 MHz, DMSO-d_6) δ 156.3, 154.3 (d, *J* = 239.5 Hz), 140.5, 139.5, 138.3, 136.0, 133.6, 129.9, 127.8, 125.4, 121.9 (d, *J* = 7.2 Hz), 116.5 (d, *J* = 23.2 Hz), 107.6 (d, *J* = 22.1 Hz), 50.0, 47.4, 46.9, 35.2, 27.2, 24.1. ESI-MS: m/z 550.8 [M-H^{+}]. HRMS (ESI) calculated for C21H22BrFN6O4S [M+H^{+}]: 553.0663; found: 553.0678.

***N*-(3-bromo-4-fluorophenyl)-*N*'-hydroxy-4-(((trans-3-(sulfamoylamino)cyclohexy**

l)methyl)amino)-1,2,5-oxadiazole-3-carboximidamide (18)

White solid (yield: 58%). HPLC purity: 95.71%. m.p.: 84 - 86 ^{o}C. ^{1}H NMR (500 MHz, DMSO-d_6) δ 11.47 (s, 1H), 8.87 (s, 1H), 7.19 (t, *J* = 8.8 Hz, 1H), 7.13 (dd, *J* = 6.0, 2.7 Hz, 1H), 6.78 (ddd, *J* = 9.0, 4.2, 2.7 Hz, 1H), 6.43 (s, 2H), 6.40 (d, *J* = 6.3 Hz, 1H), 6.15 (t, *J* = 6.0 Hz, 1H), 3.47 (q, J = 4.8 Hz, 1H), 3.18 (d, *J* = 4.0 Hz, 2H), 3.09 (t, *J* = 6.5 Hz, 1H), 2.06 – 1.94 (m, 1H), 1.77 – 1.69 (m, 1H), 1.69 – 1.61 (m, 1H), 1.60 – 1.48 (m, 2H), 1.47 – 1.39 (m, 1H), 1.30 (ddd, *J* = 13.3, 9.7, 3.6 Hz, 1H), 1.02 (qd, *J* = 11.3, 9.9, 5.3 Hz, 1H). ^{13}C NMR (125 MHz, DMSO-d_6) δ 156.3, 154.2 (d, *J* = 239.5 Hz) , 140.3, 139.8, 138.4, 125.4, 122.0 (d, *J* = 6.9 Hz), 116.4 (d, *J* = 22.9 Hz), 107.5 (d, *J* = 22.4 Hz), 49.5, 48.4, 35.6, 31.7, 31.5, 29.1, 20.0. ESI-MS: m/z 503.8 [M-H^{+}]. HRMS (ESI) calculated for C16H21BrFN7O4S [M+H^{+}]: 506.0616; found: 506.0608.

***N*-(3-bromo-4-fluorophenyl)-*N*'-hydroxy-4-((2-(1-sulfamoylpiperidin-3-yl)ethyl)amino)-1,2,5-oxadiazole-3-carboximidamide (19)**

White solid (yield: 63%). HPLC purity: 96.34%. m.p.: 59 - 61 ^{o}C. ^{1}H NMR (500 MHz, DMSO-d_6) δ 11.46 (s, 1H), 8.87 (s, 1H), 7.18 (t, *J* = 8.7 Hz, 1H), 7.12 (dd, *J* = 6.1, 2.7 Hz, 1H), 6.79 (ddd, *J* = 8.9, 4.1, 2.7 Hz, 1H), 6.68 (s, 2H), 6.19 (t, *J* = 5.7 Hz, 1H), 3.38 – 3.30 (m, 2H), 3.25 (q, *J* = 6.8 Hz, 2H), 2.51-2.57 (m, 1H), 2.28 (t, *J* = 10.7 Hz, 1H), 1.73 (td, *J* = 13.8, 4.0 Hz, 2H), 1.67 – 1.42 (m, 4H), 1.05 – 0.90 (m, 1H). ^{13}C NMR (125 MHz, DMSO-d_6) δ 156.1 , 154.3 (d, *J* = 239.5 Hz), 140.41, 139.7 138.4 (d, *J* = 2.8 Hz), 125.4 , 122.0 (d, *J* = 7.0 Hz), 116.4 (d, *J* = 23.2 Hz), 107.5 (d, *J* = 22.0 Hz), 51.9 , 46.9 , 41.9 , 32.8 , 32.7 , 29.9 , 24.2. ESI-MS: m/z 503.9 [M-H]$^{-}$. HRMS (ESI) calculated for C16H21BrFN7O4S [M+H+]: 506.0616; found: 506.0623.

***N*-(3-bromo-4-fluorophenyl)-*N*'-hydroxy-4-(((1-sulfamoylpyrrolidin-3-yl)methyl)amino)-1,2,5-oxadiazole-3-carboximidamide (20)**

White solid (yield: 57%). HPLC purity: 99.14%. m.p.: 112 - 115 ^{o}C.^{1}H NMR (400 MHz, DMSO-d_6) δ 11.44 (s, 1H), 8.90 (s, 1H), 7.17 (t, *J* = 8.8 Hz, 1H), 7.10 (dd, *J* = 6.2, 2.7 Hz, 1H), 6.81 – 6.66 (m, 3H), 6.36 (t, *J* = 5.8 Hz, 1H), 3.20 (tq, *J* = 11.5, 6.4, 5.2 Hz, 4H), 3.13 – 3.03 (m, 1H), 2.86 (dd, *J* = 10.0, 6.5 Hz, 1H), 2.53 (d, *J* = 7.3 Hz, 1H), 1.90 (h, *J* = 6.6 Hz, 1H), 1.55 (dq, *J* = 14.9, 7.6 Hz, 1H). ^{13}C NMR (125 MHz,

DMSO-d_6) δ 156.2, 154.3 (d, *J* = 239.5 Hz), 140.4, 139.6, 138.4 (d, *J* = 2.8 Hz), 125.4, 122.0 (d, *J* = 7.1 Hz), 116.5 (d, *J* = 23.1 Hz), 107.5 (d, *J* = 22.1 Hz), 51.5, 47.5, 47.1, 37.8, 29.0. ESI-MS: m/z 475.9 [M-H$^+$]. HRMS (ESI) calculated for C14H17BrFN7O4S [M-H$^+$]: 476.0157; found: 476.0153.

_N_-(3-bromo-4-fluorophenyl)-_N'_-hydroxy-4-(((1-(methylsulfonyl)pyrrolidin-2-yl) methyl)amino)-1,2,5-oxadiazole-3-carboximidamide (21)

White solid (yield: 53%). HPLC purity: 97.64%. m.p.: 77 - 79 ^{o}C. ^{1}H NMR (600 MHz, DMSO-d_6) δ 11.49 (s, 1H), 8.89 (s, 1H), 7.18 (t, *J* = 8.7 Hz, 1H), 7.13 (dd, *J* = 6.1, 2.7 Hz, 1H), 6.78 (dt, *J* = 8.9, 3.4 Hz, 1H), 6.27 (t, *J* = 6.2 Hz, 1H), 3.90 (dt, *J* = 6.7, 3.2 Hz, 1H), 3.58-3.56 (m, 1H),3.33 – 3.22 (m, 3H), 2.91 (s, 3H), 2.01 – 1.79 (m, 3H), 1.71 (dt, *J* = 11.1, 5.1 Hz, 1H). ^{13}C NMR (150 MHz, DMSO-d_6) δ 156.3, 154.2 (d, *J* = 239.5 Hz), 140.4, 139.8, 138.5 (d, *J* = 2.7 Hz), 125.4, 122.0 (d, *J* = 6.9 Hz), 116.4 (d, *J* = 23.1 Hz), 107.5 (d, *J* = 22.0 Hz), 58.5, 49.4, 48.6, 34.2, 29.2, 24.3. ESI-MS: m/z 474.9 [M-H]$^-$. HRMS (ESI) calculated for C15H18BrFN6O4S [M-H$^+$]: 475.0205; found: 475.0202.

_N_-(3-bromo-4-fluorophenyl)-_N'_-hydroxy-4-(((1-(methylsulfonyl)pyrrolidin-3-yl) methyl)amino)-1,2,5-oxadiazole-3-carboximidamide (22)

White solid (yield: 46%). HPLC purity: 99.48%. m.p.: 98 - 100 ^{o}C. ^{1}H NMR (500 MHz, Acetone-d_6) δ 10.31 (d, *J* = 1.3 Hz, 1H), 7.83 (s, 1H), 7.01 (dd, *J* = 6.0, 2.7 Hz, 1H), 6.73 (ddd, *J* = 8.9, 4.2, 2.7 Hz, 1H), 5.99 (t, *J* = 6.0 Hz, 1H), 3.26 – 2.98 (m, 5H), 2.92 – 2.80 (m, 1H), 2.59 (s, 3H), 2.45 (p, *J* = 7.2 Hz, 1H), 1.84 (dtd, *J* = 12.2, 7.3, 4.7 Hz, 1H), 1.50 (dq, *J* = 12.5, 7.8 Hz, 1H). ^{13}C NMR (125 MHz, Acetone-d_6) δ 156.1, 154.5 (d, *J* = 239.5 Hz), 140.8, 139.2, 137.7 (d, *J* = 3.2 Hz), 126.7, 123.1 (d, *J* = 7.1 Hz), 115.8 (d, *J* = 23.2 Hz), 107.3 (d, *J* = 22.2 Hz), 51.0, 47.0, 46.5, 38.2, 32.9, 28.9. ESI-MS: m/z 474.8 [M-H]$^-$. HRMS (ESI) calculated for C15H18BrFN6O4S [M+H$^+$]: 477.0350; found: 477.0356.

(_S_)-_N_-(3-bromo-4-fluorophenyl)-_N'_-hydroxy-4-(((1-sulfamoylpyrrolidin-3-yl)met hyl)amino)-1,2,5-oxadiazole-3-carboximidamide (23)

White solid (yield: 39%). HPLC purity: 97.57%. m.p.: 126 – 128 ^{o}C.^{1}H NMR (500 MHz, DMSO-d_6) δ 11.38 (s, 1H), 8.76 (s, 1H), 7.05 (t, *J* = 8.8 Hz, 1H), 7.00 (dd, *J* =

6.0, 2.7 Hz, 1H), 6.67 (ddd, *J* = 8.9, 4.2, 2.7 Hz, 1H), 6.62 (s, 2H), 6.26 (t, *J* = 5.9 Hz, 1H), 3.15 (dd, *J* = 10.0, 7.5 Hz, 1H), 3.03-3.17 (m, 3H), 3.01 (dt, *J* = 9.8, 7.5 Hz, 1H), 2.78 (dd, *J* = 10.0, 6.6 Hz, 1H), 2.43 (p, *J* = 7.3 Hz, 1H), 1.82 (dtd, *J* = 12.3, 7.3, 4.9 Hz, 1H), 1.46 (dq, *J* = 12.6, 7.6 Hz, 1H). ^{13}C NMR (125 MHz, DMSO-d_6) δ 156.2 , 154.3 (d, *J* = 239.5 Hz), 140.4, 139.6, 138.4 (d, *J* = 2.8 Hz), 125.4 , 122.0 (d, *J* = 7.1 Hz), 116.4 (d, *J* = 23.0 Hz), 107.5 (d, *J* = 22.0 Hz), 51.5 , 47.5, 47.1, 37.8, 29.0. ESI-MS: m/z 475.9 [M-H]$^-$. HRMS (ESI) calculated for C14H17BrFN7O4S [M-H$^+$]: 476.0157; found: 476.0159.

(*R*)-*N*-(3-bromo-4-fluorophenyl)-*N*'-hydroxy-4-(((1-sulfamoylpyrrolidin-3-yl)methyl)amino)-1,2,5-oxadiazole-3-carboximidamide (24)

White solid (yield: 63%). HPLC purity: 98.89%. m.p. : 124 – 127 ^{o}C.^{1}H NMR (600 MHz, DMSO-d_6) δ 11.49 (s, 1H), 8.90 (s, 1H), 7.16 (t, *J* = 8.8 Hz, 1H), 7.10 (dd, *J* = 6.1, 2.7 Hz, 1H), 6.76 (ddd, *J* = 8.9, 4.2, 2.7 Hz, 1H), 6.73 (s, 2H), 6.38 (t, *J* = 5.9 Hz, 1H), 3.25 (dd, *J* = 10.0, 7.4 Hz, 1H), 3.19 (ddd, *J* = 14.0, 7.7, 5.5 Hz, 3H), 3.10 (dt, *J* = 9.8, 7.6 Hz, 1H), 2.87 (dd, *J* = 10.0, 6.7 Hz, 1H), 2.53 (dt, *J* = 14.6, 7.3 Hz, 1H), 1.91 (dtd, *J* = 12.3, 7.3, 4.9 Hz, 1H), 1.56 (dq, *J* = 12.4, 7.7 Hz, 1H). ^{13}C NMR (150 MHz, DMSO-d_6) δ 156.2, 154.3 (d, *J* = 239.5 Hz), 140.4, 139.6, 138.4 (d, *J* = 2.8 Hz), 125.4, 122.0 (d, *J* = 7.0 Hz), 116.5 (d, *J* = 23.3 Hz), 107.6 (d, *J* = 22.0 Hz), 51.5, 47.5, 47.1, 37.8, 29.0. ESI-MS: m/z 475.9 [M-H]$^-$. HRMS (ESI) calculated for C14H17BrFN6O4S [M-H$^+$]: 476.0157; found: 476.0159.

(*S*)-*N*-(3-bromo-4-fluorophenyl)-*N*'-hydroxy-4-(((1-sulfamoylpiperidin-3-yl)methyl)amino)-1,2,5-oxadiazole-3-carboximidamide (25)

White solid (yield: 56%). HPLC purity: 99.63%. m.p.： 149 - 151 ^{o}C. ^{1}H NMR (500 MHz, DMSO-d_6) δ 11.50 (s, 1H), 8.88 (s, 1H), 7.18 (t, *J* = 8.8 Hz, 1H), 7.13 (dd, *J* = 6.1, 2.7 Hz, 1H), 6.77 (ddd, *J* = 8.9, 4.1, 2.7 Hz, 1H), 6.71 (s, 2H), 6.29 (t, *J* = 6.0 Hz,

1H), 3.39-3.49 (m, 1H), 3.33 (dd, *J* = 10.2, 5.5 Hz, 1H), 3.15 (t, *J* = 6.8 Hz, 2H), 2.54 (dd, *J* = 11.5, 3.0 Hz, 1H), 2.32 (t, *J* = 10.7 Hz, 1H), 1.93 (ddq, *J* = 10.4, 7.2, 3.6 Hz, 1H), 1.73 (dt, *J* = 13.3, 3.6 Hz, 1H), 1.64 (dt, *J* = 12.4, 4.0 Hz, 1H), 1.46 (tdd, *J* = 15.2, 7.7, 3.9 Hz, 1H), 1.10 – 0.94 (m, 1H). ^{13}C NMR (125 MHz, DMSO-d_6) δ 156.3 , 154.3 (d, *J* = 239.5 Hz), 140.4, 139.6, 138.4 (d, *J* = 2.7 Hz), 125.4, 122.0 (d, *J* = 6.9 Hz), 116.5 (d, *J* = 23.4 Hz), 107.6 (d, *J* = 22.0 Hz), 50.1, 47.8, 46.9, 35.0, 27.7, 24.0. ESI-MS: m/z 489.8 [M-H]$^-$. HRMS (ESI) calculated for C15H19BrFN7O4S [M-H$^+$]: 490.0314; found: 490.0319.

(*R*)-N-(3-bromo-4-fluorophenyl)-N'-hydroxy-4-(((1-sulfamoylpiperidin-3-yl)methyl)amino)-1,2,5-oxadiazole-3-carboximidamide (26)

White solid (yield: 54%). HPLC purity: 97.30%. m.p.: 153 - 155 ^{o}C. ^{1}H NMR (500 MHz, DMSO-d_6) δ 11.46 (s, 1H), 8.90 (s, 1H), 7.19 (t, *J* = 8.8 Hz, 1H), 7.13 (dd, *J* = 6.1, 2.7 Hz, 1H), 6.77 (ddd, *J* = 8.9, 4.1, 2.7 Hz, 1H), 6.71 (s, 2H), 6.28 (t, *J* = 6.0 Hz, 1H), 3.39-3.49 (m, 1H), 3.42 (dd, *J* = 11.4, 3.6 Hz, 1H), 3.15 (td, *J* = 6.6, 2.2 Hz, 2H), 2.54 (dd, *J* = 11.7, 3.0 Hz, 1H), 2.31 (t, *J* = 10.7 Hz, 1H), 1.93 (ddq, *J* = 14.1, 7.2, 3.4 Hz, 1H), 1.73 (ddd, *J* = 10.9, 7.3, 3.6 Hz, 1H), 1.65 (dd, *J* = 13.5, 4.2 Hz, 1H), 1.47 (qt, *J* = 11.0, 3.8 Hz, 1H), 1.01 (qd, *J* = 11.4, 3.8 Hz, 1H). ^{13}C NMR (125 MHz, DMSO-d_6) δ 156.3, 154.3 (d, *J* = 239.5 Hz), 140.4, 139.6, 138.4, 125.4, 122.0 (d, *J* = 7.0 Hz), 116.5 (d, *J* = 23.3 Hz), 107.6 (d, *J* = 22.0 Hz), 50.2, 47.8, 46.9, 35.1, 27.7, 24.0. ESI-MS: m/z 489.9 [M-H]$^-$. HRMS (ESI) calculated for C15H19BrFN7O4S [M-H$^+$]: 490.0314; found: 490.0317.

(*S*)-N-(3-bromo-4-fluorophenyl)-N'-hydroxy-4-(((1-sulfamoylpiperidin-2-yl)methyl)amino)-1,2,5-oxadiazole-3-carboximidamide (27)

White solid (yield: 61%). HPLC purity: 98.08%. m.p.: 78 - 80 ^{o}C. ^{1}H NMR (600 MHz, DMSO-d_6) δ 11.44 (s, 1H), 8.89 (s, 1H), 7.15 (t, *J* = 8.8 Hz, 1H), 7.13 (dd, *J* = 6.1, 2.7 Hz, 1H), 6.76 (dt, *J* = 9.1, 3.3 Hz, 1H), 6.67 (s, 2H), 6.18 (dd, *J* = 7.2, 5.0 Hz, 1H), 4.05 (dd, *J* = 9.5, 4.4 Hz, 1H), 3.51 – 3.57 (m, 2H), 3.40 (dt, *J* = 14.0, 7.3 Hz, 1H), 2.98 (td, *J* = 10.8, 5.0 Hz, 1H), 1.75 – 1.63 (m, 1H), 1.46 – 1.58 (m, 5H). ^{13}C NMR (151 MHz, DMSO-d_6) δ 156.2, 154.2 (d, *J* = 239.5 Hz), 140.4 , 139.7 , 138.4 (d, *J* =

2.8 Hz), 125.3, 122.0 (d, *J* = 6.8 Hz), 116.4 (d, *J* = 23.2 Hz), 107.6 (d, *J* = 22.0 Hz), 51.4, 43.2, 41.3, 25.2, 24.2, 19.0. ESI-MS: m/z 489.9 $[M-H]^-$. HRMS (ESI) calculated for $C_{15}H_{19}BrFN_7O_4S$ $[M+H^+]$: 492.0459; found: 492.0453.

(*S*)-*N*-(3-bromo-4-fluorophenyl)-*N*'-hydroxy-4-(((1-(methylsulfonyl)pyrrolidin-2-yl)methyl)amino)-1,2,5-oxadiazole-3-carboximidamide (28)

White solid (yield: 36%). HPLC purity: 97.34%. m.p.: 125 -127 °C. ^{1}H NMR (600 MHz, DMSO-d_6) δ 11.48 (s, 1H), 8.87 (s, 1H), 7.16 (t, *J* = 8.7 Hz, 1H), 7.12 (dd, *J* = 6.1, 2.7 Hz, 1H), 6.77 (ddd, *J* = 8.9, 4.2, 2.7 Hz, 1H), 6.26 (t, *J* = 6.2 Hz, 1H), 3.89 (tdd, *J* = 7.5, 5.5, 3.4 Hz, 1H), 3.34 (t, *J* = 5.9 Hz, 1H), 3.32 – 3.21 (m, 3H), 2.05 – 1.77 (m, 3H), 1.76 – 1.60 (m, 1H). ^{13}C NMR (150 MHz, DMSO-d_6) δ 156.3, 154.2, 140.3, 139.8, 138.5 (d, *J* = 2.7 Hz), 125.4, 122.0 (d, *J* = 7.1 Hz), 116.4 (d, *J* = 23.2 Hz), 107.5 (d, *J* = 21.9 Hz), 58.5, 49.4, 48.6, 34.2, 29.2, 24.3. ESI-MS: m/z 474.8 $[M-H^+]$. HRMS (ESI) calculated for $C_{15}H_{18}BrFN_6O_4S$ $[M-H^+]$: 475.0205; found: 475.0199.

(*R*)-*N*-(3-bromo-4-fluorophenyl)-*N*'-hydroxy-4-(((1-(methylsulfonyl)pyrrolidin-2-yl)methyl)amino)-1,2,5-oxadiazole-3-carboximidamide (29)

White solid (yield: 47%). HPLC purity: 97.96%. m.p.: 128 -131 °C. ^{1}H NMR (500 MHz, DMSO-d_6) δ 11.48 (s, 1H), 8.87 (s, 1H), 7.18 (t, *J* = 8.8 Hz, 1H), 7.14 (dd, *J* = 6.1, 2.7 Hz, 1H), 6.92 – 6.72 (m, 1H), 6.27 (t, *J* = 6.2 Hz, 1H), 3.92 (dq, *J* = 6.6, 3.3 Hz, 1H), 3.42 – 3.37 (m, 1H), 3.34 – 3.24 (m, 3H), 2.92 (s, 3H), 2.01 – 1.78 (m, 3H), 1.73 (dt, *J* = 10.5, 4.9 Hz, 1H). ^{13}C NMR (125 MHz, DMSO-d_6) δ 156.3, 154.3 (d, *J* = 239.5 Hz), 140.3, 139.8, 138.5 (d, *J* = 2.8 Hz), 125.4, 122.0 (d, *J* = 7.1 Hz), 116.4 (d, *J* = 23.1 Hz), 107.5 (d, *J* = 21.9 Hz), 58.5, 49.3, 48.6, 34.3, 29.2, 24.3. ESI-MS: m/z 474.8 $[M-H]^-$. HRMS (ESI) calculated for $C_{15}H_{18}BrFN_7O_4S$ $[M-H^+]$: 475.0205; found: 476.0212.

(*S*)-*N*-(3-bromo-4-fluorophenyl)-*N*'-hydroxy-4-(((1-(methylsulfonyl)pyrrolidin-3-

yl)methyl)amino)-1,2,5-oxadiazole-3-carboximidamide (30)

White solid (yield: 41%). HPLC purity: 99.13%. m.p.: 145 - 147 ^{o}C.^{1}H NMR (600 MHz, DMSO-d_6) δ 11.44 (s, 1H), 8.91 (s, 1H), 7.17 (t, *J* = 8.8 Hz, 1H), 7.10 (dd, *J* = 6.1, 2.7 Hz, 1H), 6.76 (ddd, *J* = 8.9, 4.2, 2.7 Hz, 1H), 6.39 (t, *J* = 5.9 Hz, 1H), 3.33 – 3.28 (m, 2H), 3.21 (dtd, *J* = 14.1, 7.4, 6.7, 3.2 Hz, 3H), 2.95 (dd, *J* = 10.0, 6.9 Hz, 1H), 2.88 (s, 3H), 2.56 (p, *J* = 7.2 Hz, 1H), 1.94 (dtd, *J* = 12.0, 7.2, 4.9 Hz, 1H), 1.60 (dq, *J* = 12.4, 7.8 Hz, 1H). ^{13}C NMR (150 MHz, DMSO-d_6) δ 156.2, 154.3 (d, *J* = 239.5 Hz), 140.5, 139.5, 138.3, 125.4, 122.0 (d, *J* = 6.8 Hz), 116.5 (d, *J* = 23.3 Hz), 107.6 (d, *J* = 21.9 Hz), 51.3, 47.4, 46.6, 38.2, 33.6, 29.2. ESI-MS: m/z 474.8 [M-H]$^{-}$. HRMS (ESI) calculated for C15H18BrFN7O4S [M-H^{+}]: 475.0205; found: 476.0198.

(*R*)-N-(3-bromo-4-fluorophenyl)-N'-hydroxy-4-(((1-(methylsulfonyl)pyrrolidin-3-yl)methyl)amino)-1,2,5-oxadiazole-3-carboximidamide (31)

White solid (yield: 38%). HPLC purity: 97.96%. m.p.: 144 - 146 ^{o}C. ^{1}H NMR (500 MHz, DMSO-d_6) δ 11.40 (s, 1H), 8.90 (s, 1H), 7.19 (t, *J* = 8.8 Hz, 1H), 7.12 (dd, *J* = 6.2, 2.7 Hz, 1H), 6.79 (dt, *J* = 7.9, 3.4 Hz, 1H), 6.40 (t, *J* = 6.0 Hz, 1H), 3.03 - 3.35 (m, 2H), 3.19 - 3.28 (m, 3H), 2.98 (dd, *J* = 10.1, 7.0 Hz, 1H), 2.90 (s, 3H), 2.58 (hept, *J* = 6.2, 5.1 Hz, 1H), 1.98 (dt, *J* = 12.8, 6.4 Hz, 1H), 1.63 (dq, *J* = 15.3, 8.1 Hz, 1H). ^{13}C NMR (125 MHz, DMSO-d_6) δ 156.2, 154.3 (d, *J* = 239.5 Hz), 140.5, 139.6, 138.3, 125.4, 122.0 (d, J = 7.0 Hz), 116.5 (d, J = 23.4 Hz), 107.6 (d, J = 22.0 Hz), 51.3, 47.4, 46.6, 38.2, 33.7, 29.2. ESI-MS: m/z 474.8 [M-H]$^{-}$. HRMS (ESI) calculated for C15H18BrFN7O4S [M-H^{+}]: 477.0350; found: 477.0356.

(*S*)-*N*-(3-bromo-4-fluorophenyl)-*N*'-hydroxy-4-(((1-(methylsulfonyl)piperidin-3-yl)methyl)amino)-1,2,5-oxadiazole-3-carboximidamide (32)

White solid (yield: 62%). HPLC purity: 99.48%. m.p.: 150 – 152 ^{o}C. ^{1}H NMR (500 MHz, DMSO-d_6) δ 11.46 (s, 1H), 8.90 (s, 1H), 7.19 (t, *J* = 8.7 Hz, 1H), 7.13 (dd, *J* = 6.1, 2.7 Hz, 1H), 6.77 (ddd, *J* = 8.9, 4.1, 2.7 Hz, 1H), 6.31 (t, *J* = 6.0 Hz, 1H), 3.50 (dd, *J* = 11.9, 3.9 Hz, 1H), 3.42 (dd, *J* = 10.2, 5.8 Hz, 1H), 3.16 (ddt, *J* = 10.1, 6.5, 4.0 Hz, 2H), 2.84 (s, 3H), 2.71 (td, *J* = 11.3, 2.9 Hz, 1H), 2.50 – 2.46 (m, 1H), 1.92 (ddt, *J*

= 10.5, 6.8, 3.6 Hz, 1H), 1.74 (dt, *J* = 13.4, 3.7 Hz, 1H), 1.70 – 1.62 (m, 1H), 1.47 (tdd, *J* = 11.2, 8.0, 3.8 Hz, 1H), 1.12 – 0.97 (m, 1H). ^{13}C NMR (125 MHz, DMSO-d_6) δ 156.4, 154.3 (d, *J* = 239.5 Hz), 140.5, 139.5, 138.3 (d, *J* = 2.9 Hz), 125.4, 122.0 (d, *J* = 6.9 Hz), 116.5 (d, *J* = 23.3 Hz), 107.6 (d, *J* = 22.0 Hz), 49.5, 47.5, 46.4, 35.3, 34.4, 27.5, 24.3. ESI-MS: m/z 488.8 [M-H]$^-$. HRMS (ESI) calculated for C16H20BrFN6O4S [M+H$^+$]: 491.0504; found: 491.0507.

(*R*)-*N*-(3-bromo-4-fluorophenyl)-*N*'-hydroxy-4-(((1-(methylsulfonyl)piperidin-3-yl)methyl)amino)-1,2,5-oxadiazole-3-carboximidamide (33)

White solid (yield: 61%). HPLC purity: 97.69%. m.p.: 153 – 155 ^{o}C. ^{1}H NMR (500 MHz, DMSO-d_6) δ 11.49 (s, 1H), 8.90 (s, 1H), 7.18 (t, *J* = 8.7 Hz, 1H), 7.13 (dd, *J* = 6.1, 2.7 Hz, 1H), 6.77 (ddd, *J* = 8.8, 4.1, 2.7 Hz, 1H), 6.32 (t, *J* = 6.0 Hz, 1H), 3.50 (dd, *J* = 11.6, 3.7 Hz, 1H), 3.43 (d, *J* = 11.8 Hz, 1H), 3.16 (ddd, *J* = 12.8, 6.9, 4.1 Hz, 2H), 2.84 (s, 3H), 2.71 (td, *J* = 11.4, 2.9 Hz, 1H), 2.49 (d, *J* = 11.1 Hz, 1H), 1.91 (ddt, *J* = 10.3, 7.2, 3.6 Hz, 1H), 1.80 – 1.70 (m, 1H), 1.68 (dd, *J* = 13.4, 4.0 Hz, 1H), 1.46 (tdd, *J* = 14.7, 9.5, 3.8 Hz, 1H), 1.13 – 0.99 (m, 1H). ^{13}C NMR (125 MHz, DMSO-d_6) δ 156.3, 154.3 (d, *J* = 239.5 Hz), 140.5, 139.5, 138.4 (d, *J* = 2.8 Hz), 125.4 , 122.0 (d, *J* = 7.0 Hz), 116.5 (d, *J* = 23.2 Hz), 107.6 (d, *J* = 22.0 Hz), 50.0, 47.5, 46.4, 35.3, 34.4, 27.5, 24.3. ESI-MS: m/z 488.8 [M-H]$^-$. HRMS (ESI) calculated for C16H20BrFN6O4S [M-H$^+$]: 489.0361; found: 476.0351.

■ ASSOCIATED CONTENT

Supporting Information

Copies of NMR spectra and HPLC experiments. (PDF)

■ AUTHOR INFORMATION

Corresponding Authors

*H. Liu: Phone, +86-21-50807042; E-mail, hliu@simm.ac.cn.

*L. Meng: Phone, +86-21-50805315; E-mail, lhmeng@simm.ac.cn

ORCID

Hong Liu: 0000-0002-0863-7853

Author Contributions

‖X. S. and P. S. contributed equally to this study.

Notes

The authors declare no competing financial interest.

■ ACKNOWLEDGMENTS

We gratefully acknowledge the funds from National Program on Key Basic Research Project of China (2015CB910304) and the National Natural Science Foundation (81620108027, 21632008, and 21402226).

■ ABBREVIATIONS USED

IDO, Indoleamine 2,3-dioxygenase; BID, bis in die; PK, pharmacokinetics; GCN2, general regulatory repressor kinase 2; SAR, structure-activity relationship; CDI, carbonyl diimidazole; THF, tetrahydrofuran; TFA, trifluoroacetic acid; TEA, triethylamine; IC_{50}, half-maximal inhibitory concentration.

■ REFERENCES

[1] O. Takikawa, R. Yoshida, R. Kido, O. Hayaishi, Tryptophan degradation in mice initiated by indoleamine 2,3-dioxygenase, J. Biol .Chem. 261 (1986) 3648-3653.

[2] A.C. Terentis, S.R. Thomas, O. Takikawa, T.K. Littlejohn, R.J. Truscott, R.S. Armstrong, S.R. Yeh, R. Stocker, The heme environment of recombinant human indoleamine 2,3-dioxygenase. Structural properties and substrate-ligand interactions, J. Biol. Chem. 277 (2002) 15788-15794.

[3] J.M. Gostner, K. Becker, F. Uberall, D. Fuchs, The potential of targeting indoleamine 2,3-dioxygenase for cancer treatment, Expert. Opin. Ther. Targets. 19 (2015) 605-615.

[4] D.H. Munn, A.L. Mellor, Indoleamine 2,3-dioxygenase and tumor-induced tolerance, J. Clin.

Invest. 117 (2007) 1147-1154.

[5] M. Zamanakou, A.E. Germenis, V. Karanikas, Tumor immune escape mediated by indoleamine 2,3-dioxygenase, Immunol. Lett. 111 (2007) 69-75.

[6] A.L. Mellor, D.H. Munn, Tryptophan catabolism and regulation of adaptive immunity, J. Immunol. 170 (2003) 5809-5813.

[7] S. Qian, M. Zhang, Q. Chen, Y. He, W. Wang, Z. Wang, IDO as a drug target for cancer immunotherapy: recent developments in IDO inhibitors discovery, RSC Advances 6 (2016) 7575-7581.

[8] C.A. Opitz, U.M. Litzenburger, F. Sahm, M. Ott, I. Tritschler, S. Trump, T. Schumacher, L. Jestaedt, D. Schrenk, M. Weller, M. Jugold, G.J. Guillemin, C.L. Miller, C. Lutz, B. Radlwimmer, I. Lehmann, A. von Deimling, W. Wick, M. Platten, An endogenous tumour-promoting ligand of the human aryl hydrocarbon receptor, Nature 478 (2011) 197-203.

[9] D.A. Wainwright, A.L. Chang, M. Dey, I.V. Balyasnikova, C.K. Kim, A. Tobias, Y. Cheng, J.W. Kim, J. Qiao, L. Zhang, Y. Han, M.S. Lesniak, Durable therapeutic efficacy utilizing combinatorial blockade against IDO, CTLA-4, and PD-L1 in mice with brain tumors, Clin. Cancer. Res. 20 (2014) 5290-5301.

[10] H.K. Koblish, M.J. Hansbury, K.J. Bowman, G. Yang, C.L. Neilan, P.J. Haley, T.C. Burn, P. Waeltz, R.B. Sparks, E.W. Yue, A.P. Combs, P.A. Scherle, K. Vaddi, J.S. Fridman, Hydroxyamidine inhibitors of indoleamine-2,3-dioxygenase potently suppress systemic tryptophan catabolism and the growth of IDO-expressing tumors, Mol. Cancer. Ther. 9 (2010) 489-498.

[11] D. Zamarin, M.A. Postow, Immune checkpoint modulation: rational design of combination strategies, Pharmacol. Ther. 150 (2015) 23-32.

[12] A.J. Muller, G.C. Prendergast, Marrying immunotherapy with chemotherapy: why say IDO?, Cancer. Res. 65 (2005) 8065-8068.

[13] M.D. Lovelace, B. Varney, G. Sundaram, M.J. Lennon, C.K. Lim, K. Jacobs, G.J. Guillemin, B.J. Brew, Recent evidence for an expanded role of the kynurenine pathway of tryptophan metabolism in neurological diseases, Neuropharmacology 112 (2017) 373-388.

[14] M. Platten, W. Wick, B.J. Van den Eynde, Tryptophan catabolism in cancer: beyond IDO and tryptophan depletion, Cancer. Res. 72 (2012) 5435-5440.

[15] E.W. Yue, R. Sparks, P. Polam, D. Modi, B. Douty, B. Wayland, B. Glass, A. Takvorian, J. Glenn, W. Zhu, M. Bower, X. Liu, L. Leffet, Q. Wang, K.J. Bowman, M.J. Hansbury, M. Wei, Y. Li, R. Wynn, T.C. Burn, H.K. Koblish, J.S. Fridman, T. Emm, P.A. Scherle, B. Metcalf, A.P. Combs, INCB24360 (Epacadostat), a Highly Potent and Selective Indoleamine-2,3-dioxygenase 1 (IDO1) Inhibitor for Immuno-oncology, ACS Med. Chem. Lett. 8 (2017) 486-491.

[16] S. Kumar, J.P. Waldo, F.A. Jaipuri, A. Marcinowicz, C. Van Allen, J. Adams, T. Kesharwani, X. Zhang, R. Metz, A.J. Oh, S.F. Harris, M.R. Mautino, Discovery of Clinical Candidate (1R,4r)-4-((R)-2-((S)-6-Fluoro-5H-imidazo[5,1-a]isoindol-5-yl)-1-hydroxyethyl)cyc lohexan-1-ol (Navoximod), a Potent and Selective Inhibitor of Indoleamine 2,3-Dioxygenase 1, J. Med. Chem. 62 (2019) 6705-6733.

[17] J.E. Cheong, A. Ekkati, L. Sun, A patent review of IDO1 inhibitors for cancer, Expert. Opin. Ther. Pat. 28 (2018) 317-330.

[18] S. Crosignani, P. Bingham, P. Bottemanne, H. Cannelle, S. Cauwenberghs, M. Cordonnier, D. Dalvie, F. Deroose, J.L. Feng, B. Gomes, S. Greasley, S.E. Kaiser, M. Kraus, M. Negrerie, K. Maegley, N. Miller, B.W. Murray, M. Schneider, J. Soloweij, A.E. Stewart, J. Tumang, V.R. Torti, B. Van Den Eynde, M. Wythes, Discovery of a Novel and Selective Indoleamine 2,3-Dioxygenase (IDO-1) Inhibitor 3-(5-Fluoro-1H-indol-3-yl)pyrrolidine-2,5-dione (EOS200271/PF-06840003) and Its Characterization as a Potential Clinical Candidate, J. Med. Chem. 60 (2017) 9617-9629.

[19] S. Yang, X. Li, F. Hu, Y. Li, Y. Yang, J. Yan, C. Kuang, Q. Yang, Discovery of tryptanthrin derivatives as potent inhibitors of indoleamine 2,3-dioxygenase with therapeutic activity in Lewis lung cancer (LLC) tumor-bearing mice, J. Med. Chem. 56 (2013) 8321-8331.

[20] S.Y. Lin, T.K. Yeh, C.C. Kuo, J.S. Song, M.F. Cheng, F.Y. Liao, M.W. Chao, H.L. Huang, Y.L. Chen, C.Y. Yang, M.H. Wu, C.L. Hsieh, W. Hsiao, Y.H. Peng, J.S. Wu, L.M. Lin, M. Sun, Y.S. Chao, C. Shih, S.Y. Wu, S.L. Pan, M.S. Hung, S.H. Ueng, Phenyl Benzenesulfonylhydrazides Exhibit Selective Indoleamine 2,3-Dioxygenase Inhibition with Potent in Vivo Pharmacodynamic Activity and Antitumor Efficacy, J. Med. Chem. 59 (2016) 419-430.

[21] G.V. Long, R. Dummer, O. Hamid, T.F. Gajewski, C. Caglevic, S. Dalle, A. Arance, M.S. Carlino, J.J. Grob, T.M. Kim, L. Demidov, C. Robert, J. Larkin, J.R. Anderson, J. Maleski, M. Jones, S.J. Diede, T.C. Mitchell, Epacadostat plus pembrolizumab versus placebo plus pembrolizumab in patients with unresectable or metastatic melanoma

(ECHO-301/KEYNOTE-252): a phase 3, randomised, double-blind study, Lancet. Oncol. 20 (2019) 1083-1097.

[22] J. Boer, R. Young-Sciame, F. Lee, K.J. Bowman, X. Yang, J.G. Shi, F.M. Nedza, W. Frietze, L. Galya, A.P. Combs, S. Yeleswaram, S. Diamond, Roles of UGT, P450, and Gut Microbiota in the Metabolism of Epacadostat in Humans, Drug. Metab. Dispos. 44 (2016) 1668-1674.

[23] A. Lewis-Ballester, K.N. Pham, D. Batabyal, S. Karkashon, J.B. Bonanno, T.L. Poulos, S.R. Yeh, Structural insights into substrate and inhibitor binding sites in human indoleamine 2,3-dioxygenase 1, Nat. Commun. 8 (2017) 1693.

[24] C.J. Yu, M.F. Zheng, C.X. Kuang, W.D. Huang, Q. Yang, Oren-gedoku-to and its constituents with therapeutic potential in Alzheimer's disease inhibit indoleamine 2, 3-dioxygenase activity in vitro, Journal of Alzheimer's disease : JAD 22 (2010) 257-266.

[25] Schwaid, A.G. and I. Cornella-Taracido, Causes and Significance of Increased Compound Potency in Cellular or Physiological Contexts. J. Med. Chem. 61 (2018) 1767-1773.

[26] Munn, D.H., et al., GCN2 Kinase in T Cells Mediates Proliferative Arrest and Anergy Induction in Response to Indoleamine 2,3-Dioxygenase. Immunity. 22 (2005) 633-642.

[27] T. Stutchbury, O. Takikawa, D. Skylas, J. Jamie, M. Walker, R. J.W. Truscott, Expression and Purification of Recombinant Human Indoleamine 2,3-Dioxygenase, Protein Expression and Purification 19 (2000) 22-29.

The authors declare no competing financial interest.